Study on the effects of intercellular radiosensitivity uncertainty using a biophysical model in radiotherapy

(放射線治療における生物物理モデルによる細胞間放射線感受性の不確かさの影響に関する研究)

March　２０１６

College of Life and Materials Systems Engineering

Graduate School of Advanced Technology and Science

Tokushima University

Masataka Oita

Abstract

放射線治療は，手術，化学療法と並んで主要な治療手段として発展してきた。近年，がん治療患者の半数以上が一連の治療過程において放射線治療を受けている。加えて，放射線治療は長年にわたって根治的な治療手段としてのみならず，緩和的な治療手段として実践されてきた。放射線治療の理論的な研究は，古くから放射線生物学に基づく基礎実験の結果とともに発展し，とりわけ放射線に対する細胞応答に関する機序解明が重要とされてきた。近年の分子生物学の発展に伴い，放射線に対する細胞の分子生物学的な作用機序が次第に解明されつつある。しかし，放射線生物学を視野に入れた放射線治療効果の改善ならびに臨床応用に関しては多くの課題が残されている。

X 線の発見以来，放射線治療は 120 年近い歴史があるが，その生物学的影響やプロセスは非常に複雑であり，臨床では組織反応の定量化（NSD や TDF）が治療成績改善に重要な役割を果たしてきた。1980 年代以降，より正確な放射線治療効果の評価や予測において LQ モデルが提唱され，現在もなお臨床で幅広く応用されている。しかし，低酸素細胞や腫瘍幹細胞の存在，空間，時間的に不均一な放射線照射，バイスタンダー効果，細胞周期，遺伝子変異等に伴う放射線感受性の違いに対する課題が残されている。

本研究では，様々な環境下における細胞間放射線感受性の不確かさを定量的に評価し，また臨床の放射線治療ではどの程度影響しうるのか，治療計画を通じて応用可能とすることを目標とする。しかし，この目標を全て達成するには，細胞の放射線感受性は，細胞特性（細胞周期，細胞生存環境，病理組織の違い，遺伝子タイプ等）および放射線特性（線種，線質，線量率（照射時間），線量分布）の違いによってどのように影響するのか解明することが重要とされる。

本研究では，幾つかの制限を設けた上で，乳がんマウス由来のEMT6細胞を用いて基礎実験を行い，生存環境（酸素分圧）の違いに伴う放射線感受性の変化についてLQモデルを利用して解析した。方法は，培養したEMT6細胞（2×10^6 cells）を試験管に入れ，常酸素群，低酸素群として異なる放射線量（4 Gy-28 Gy）でX線照射（150 kV，4 Gy/min）した。このとき，低酸素細胞は，95 %窒素，5 %二酸化炭素の混合ガスを30分曝露させて作成した。また，低酸素群に増感剤（etanidazole）を加えた群についても，同様に実験し，コロニーアッセイを行い，細胞生存率曲線から生物物理モデルパラメータ（α成分，β成分，D_{50}，γ）を導出した。解析結果から，α成分のパラメータ（平均値±1標準偏差）は，常酸素細胞，低酸素細胞，低酸素細胞に増感剤を加えたもので，それぞれ0.257 ± 0.188 Gy^{-1}，0.078 ± 0.080 Gy^{-1}，0.182 ± 0.116 Gy^{-1}となった。同様に，β成分の

パラメータは，それぞれ0.0159 ± 0.0208 Gy^{-2}，0.0076 ± 0.0113 Gy^{-2}，　0.0062 ± 0.0077 Gy^{-2}となった。D_{50}パラメータは，それぞれ3.2 ± 2.5 Gy，6.4 ± 2.7 Gy，3.7 ± 1.4 Gyとなった。αおよびD_{50}の値は明らかに常酸素群と低酸素群で異なり，また同一群でも多少のばらつきを持ち，生存環境の違いだけでなく，同じ環境の細胞間でも放射線感受性は大きく変動することが明らかとなった。

続いて，上記の課題に対する検討として，臨床で用いられる 3 次元治療計画装置（Eclipse ver.11.0，Varian medical systems，US）においてファントムおよび患者模擬データによる臨床治療計画から，腫瘍パラメータであるα/β比，γ，D_{50}の違いや変動が腫瘍局所制御率（TCP）に，また正常臓器パラメータであるのα/β比，n 値，m 値が正常臓器副作用発生率（NTCP）にどのような影響を及ぼすかを検討した。このとき，治療ビームは臨床で用いられている 6 MV X 線のデータ（Novalis-Tx，BrainLab，US)を利用した。線量分割スケジュールは，70 Gy/35 fr，72 Gy/36 fr，74 Gy/37 fr，76 Gy/38 fr，78 Gy/39 fr，72 Gy/40 fr，73.8 Gy/41 fr，45.6 Gy/42 fr，77.4 Gy/43 fr，79.2 Gy/44 fr，81 Gy/45 fr，52.5 Gy/20 fr，57 Gy/19 fr，60 Gy/20 fr，62 Gy/20 fr，56 Gy/16 fr，63.2 Gy/20 fr，66 Gy/22 fr，35 Gy/5 fr，37.5 Gy/5 fr，40 Gy/5 fr による複数パターンで解析を行い，すべて，1 日 1 回による週 5 日間照射を想定した。また，解析の際，線量分割スケジュールの違いを考慮するため生物学的等価線量（BED）を用い

た。結果として，腫瘍の TCP は BED_{10}（通常，腫瘍に対する生物学的等価線量とされる）に依存して増加し，α/β比，γ，D_{50}はいずれも値が小さいほど低下する傾向があった。α/β比，γ，D_{50}の変動に対する TCP の影響は，α/β比，γに比べてD_{50}の方が強く生じた。正常臓器の NTCP は BED_3（通常，正常臓器に対する生物学的等価線量とされる）に依存して増加し，m 値が大きいほど，n 値が小さいほど上昇する傾向があった。α/β比，m 値， n 値の変動に対する NTCP の影響は，高線量寡分割プロトコルにおいて m 値，n 値に比べてα/β比の方が強く生じた。これらの結果から，腫瘍および正常臓器への影響は，線量分割スケジュールの違い，生物学的パラメータの値や変動に依存することが明らかとなり，基礎実験で得られた知見とともに更なる治療計画の最適化へのアプローチに向けて応用可能な結果が得られた。

本研究では，提案手法に基づいて，乳がんマウス由来の EMT6/KU 細胞を用いて基礎実験を行い，生存環境（酸素分圧）の違いに伴う放射線感受性の変化について解析した。また，それらの結果を踏まえて，臨床治療計画において，生物物理モデルを適用し，各種パラメータ値の変動を加味した治療効果予測について提案した。治療効果予測が可能な生物物理モデルを用いた臨床治療計画の最適化は，個別化治療（テーラーメイド医療）において重要とされる，しかし，結果が示すようにパラメータ値の信頼性に強く依存して予測結果は変化す

るため，パラメータ値の決定精度（各種検査法）の確立とともに，不確かさを含む評価法もまた重要であることが明らかとなった。

Contents

List of Figures

List of Tables

Chapter 1

Introduction

Radiotherapy has developed as primary treatment options for cancer along with surgery and chemotherapy. Recently, more than half of all cancer patients have receiving radiation therapy during their course of illness (1, 2). In addition to the radical therapeutic use of radiotherapy, many patients have been received palliative treatment by radiation therapy for many years.

Theoretical studies based on the *in vitro* experiments in radiobiology have contributed to the development of radiotherapy. There is obvious that radiobiology has developed with valuable data on its mechanisms of effects of cells by radiation. However, few of these still have led to demonstrable clinical gains. In the field of clinical radiotherapy, the conversion formulae based on the linear quadratic (LQ) equation (3) often has been used in the choice of specific protocols. However, the equation also has been limited by the inadequacy of the theoretical and experimental models so that it always needs to rely on the results of clinical trials.

Ionizing radiation consisting of high energy photons and electrons produced by 4-21 MV linear accelerator is the most commonly used for the radiotherapy in a clinical situation. Range from less than 100 keV to order of MeV electrons arose from the molecules within cells, which is in the body through the interactions with the incident ionizing radiation, cause most of the biological damage known as DNA breakage, cell killing (apoptosis) and so on. However, for many years, little attention was paid towards differences in the mechanisms or types of cell death after irradiation. Because cell death itself is typically very hard to assess, quantification of cell death by ionizing radiation is highly complicated by the fact that cells die at various times after irradiation, and sometimes surviving cells continue to proliferate. Many researchers have focused on assessing clonogenic cell survival, which specifies as the ability of a cell to proliferate indefinitely after irradiation. From a macroscopic viewpoint, it can be clear that the surviving cells would decrease by a certain amount of radiation dose. In contrast, it is challenging that from a microscopic viewpoint, no one still predict which cell die or survive by radiation. These uncertain phenomena would be needed a much more robust and relevant parameter to

assess radiation effect stochastically since any cell that retains proliferative capacity can cause failure to cancer treatment.

Consequently, it has well known that by far the most efficient way of improving the outcome of the treatment is to practice the quality assurance for the precise prescription of radiation dose and the delivery techniques to the localized tumour. These developments undoubtedly lead to further improvements in tumour control rates and reductions in morbidity. However, it is critical to consider not only the specific types of cell death that lead to the destruction of the cell but also to evaluate the uncertainties of cell death or cell survival by radiation. In this thesis, we investigate the distribution of uncertainty of cell survival due to radiation and application of treatment planning.

Chapter 2

Definition of radiation effects and biophysical models

2-1. Radiation effects

2-1-1. The time frames for effects of radiation

The irradiation effects of radiation to any biological system generate several processes that differ considerably from the time frames (4, 5) are mainly divided into three processes (Figure 1).

The first, the physical process consists of interactions between charged particles and the atoms composed of molecules in tissue. A charged particles, which are commonly secondary electrons produced in the body by a high energy photon beam in modern clinical radiotherapy, takes about 10^{-18} second to traverse the DNA molecule in tissue and about 10^{-14} second to pass through a cell. If these charged particles are sufficiently energetic, they interact mainly with orbital electrons within an atom (i.e. it make excitation or ionization) in a cell and occur a cascade of ionization events. For 1 Gy of radiation absorbed dose, there are more than 10^5 ionizations within the volume of every cell of diameter, which is about 10 μm.

The second, the chemical process consists of the period in which these ionized and excited atoms/molecules interact with other cells as a chemical reaction. Ionization and excitation of orbital electrons in atoms and molecules cause the cut of chemical bonds of them and the isolated molecules known as free radicals form simultaneously. Free radical are highly reactive, and their reactions complete within approximately 1 ms (millisecond) of radiation exposure.

The third, the biological process consists of all subsequent processes after chemical phases, such as repair processes, further cell divisions, mitotic death, apoptosis, effects on organs and carcinogenesis. These subsequent processes begin with enzymatic reactions of that act on the repair of residual chemical damage by radiation. Double-strand breaks (DSB) are more frequent in radiation-induced damage than single strand breaks (SSB), which are more often in normal DNA damage. In the case of small doses of radiation exposure, most of the damages in DSB are repaired. However, some lesions would fail to repair of DSB and to lead to mutations or loss of genetic information or cell death as higher doses of radiation exposure. The subsequent unrepairable damages in DSBs would cause the

early symptoms as normal tissue response from several weeks after radiation exposure. More than several months after irradiation, delayed reactions might appear as more serious damages of organs including second cancers (i.e. radiation carcinogenesis).

2-1-2. Dose response curves of cells by radiation

The response of radiation damage in irradiated normal tissue increases as the amount of radiation dose, and it has a peak and decline (dotted line in Figure 2a). The appearance of the peak changes with radiation dose and dose rate so that this would lead to temporal uncertainties of the response in the tissue. Some early tissue responses show a trend of the cumulative curve that has a plateau, and the height of the plateau is a good index of the total response to the tumour and the normal tissue. Meanwhile, the delayed tissue responses are dynamic so that the cumulative curve would creep up even after irradiation. Cell survival curves are further examples of dose-response curves that often present in the result of fundamental experiments in radiobiology. The shape of the curve on the dose scale indicates the radiation sensitivity of the cells in the tumour and normal tissue. The steepness of the curve also indicates the absolute change in

response, which accompany an increase or decrease in radiation dose as characteristics of radiation sensitivity.

It is a well-known fact that in radiation therapy that multiple fractionated radiation doses irradiated over a period of a few weeks in common result a better therapeutic response than single fraction dose. Experimentally, altered dose fractionation (e.g. number of fractionation or fraction size, dose rate) in multiple studies demonstrated the different therapeutic effect regarding an iso-effect. The iso-effect means how the total radiation dose for the chosen level of effect varies with dose schedule with consideration of some upper limit of tolerance of the tissue (6, 7).

2-1-3. The approach to cancer therapy by radiation

If the curve for tumour response is much superior to that for normal tissue, there is a therapeutic advantage by radiation. As the prescription dose increase, not only the tumour but the normal tissue response is expected to rise. If we can control the tumour and the normal tissue response, sigmoid relationships to the amount of dose would be formed (Figure 2b). The relative shift of the response curves for the tumour and normal tissues should usually be different. However, to minimize the normal tissue damage

considering with tolerance level, the response curves between tumour and normal tissue should be interspatial combined with drug or state of the art irradiation techniques. The concept of cancer therapy by radiation is to optimize the tumour control dose and the tolerance dose in normal tissue spatially and temporarily (i.e. total dose, the number of fractionation and dose rate).

2-1-4. Radiation-induced DNA damage

Ionizing radiation consisting of electromagnetic radiation, usually photons and electrons, is most commonly used in the treatment of patients with radiotherapy. The maximum energy of 4-10 MV photons produced by the acceleration of electrons using a linear accelerator that typically used in Japanese radiotherapy departments. The major effects of the radiation are its ability to ionize, or eject electrons, from atoms and molecules within cells of which it composes the tumour and the normal tissues. Most biological damage in the cell caused by the ejected electrons that arise further ionizations in molecules until they slow down and stop. At the termination of the end tracks, electron interactions with other molecules become more frequent and cause clusters of ionizations. Some of the clusters directly

occur in DNA of a cell, and the cell loses function to repair the damage (Figure 3).

Ionized molecules of water inside cells produced by electrons are very reactive and can lead to the breaking of chemical bonds. This phenomenon can also disrupt the structure of DNA, which may cause severe damages if not repaired adequately at the time. The result of permanent damage to DNA can be often fatal for the cell. Cellular DNA comprises two opposing strands linked by hydrogen bonds and forming a double helical structure. Each strand composed of a linear chain of the four bases, adenine (A), cytosine (C), guanine (G) and thymine (T). Some reports show that a radiation dose of one gray (1 Gy) produces 10^5 ionizations per cell, which cause about 1000-2000 DNA initial single strand breaks (SSBs) and 25-40 DNA initial double strand breaks (DSBs) (8, 9).

Because of the functional importance of DNA, the cells and the organisms have developed a complex series of processes and signal pathways for repairing those inside of DNAs from oxidation and ionizing radiation (10). These include different forms of DNA repair such as base excision repair (BER), single-strand break repair (SSBR), double strand breaks repair of

homologous recombination (HR) and non-homologous end-joining (NHEJ). This kind of repair forms has coped with the different forms of DNA damage induced by various agents.

2-1-5. Induction of cell death and repair after irradiation

The treatment of radiotherapy is to cause the death of individual tumour cells in the malignant lesion. The radiobiological effects of cell death are considerably affected by radiation dose and signal pathways within the cellular response including DNA damage by radiation. Because of differences between the types of cells, the eventual cell death can also different among those cell types. Quantification of cell death is highly complicated because the cells die at various timing after irradiation such one or two cycles around their specific cell cycle. Instead, the rest of surviving cells continue to proliferate. However, it is clear that radiation can kill cells by various mechanisms. Apoptosis, well known as a programmed form of cell death by radiation, results in self-destruction and removal of the cell (11). Also, these genetically controlled programs and several other pathways under genetic control have been identified such as autophagy, senescence, and necrosis that contribute to preventing further proliferation (12).

2-2. Biophysical models

2-2-1. Target theory

The prediction how radiation might kill cell is an important issue in specific targets accounting for the measurement of radiation sensitivity of the cell or results of radiotherapy. Historically, there are two versions of target theories that had used as classic calculation models. The first theory is that just one hit by radiation on a single sensitive target would lead to the death of the cell (i.e. it is called single target single hit model). In this theory, the cell survival exponentially decreased. Using Poisson statistics, we can define the probability (p) of cell survival during irradiation with many hits on different cells by the following equation (Figure 4a).

$$p\,(\text{survival}) = p\,(0\ \text{hits}) = e^{(-D/D_0)} \qquad (2.1)$$

where D_0 means the dose that gives an average of one hit per target. D/D_0 means the average number of hits per target. In semi-logarithmic plot, this curves show straight line and they are usually found for the inactivation of viruses and bacteria, however they can fit only for some very sensitive mammalian cells or in case of using high LET radiations.

The second theory is that the cell survival curves have some shoulder to fit

mammalian cells' survival curve, which called multi-target single hit model. In this extended model, just one hit by radiation on each of n targets in the cell is required for death of the cell. Similar to the equation (2.1), using Poisson statistics, we can define the probability (p) of cell survival during irradiation by the following equation according to some hypothesizes (Figure 4b).

$$p\,(0 \text{ hits on a specific target}) = e^{(-D/D_0)} \tag{2.2}$$

Then

$$p\,(\text{specific target inactivated}) = 1 - e^{(-D/D_0)} \tag{2.3}$$

If there are n targets in the cell,

$$p\,(\text{all n target inactivated}) = \left\{1 - e^{(-D/D_0)}\right\}^n \tag{2.4}$$

Therefore,

$$p\,(\text{not all targets inactivated}) = 1 - \left\{1 - e^{(-D/D_0)}\right\}^n \tag{2.5}$$

where multi-target single hit survival curves have a shoulder so that the quasi-threshold dose (D_q) is defined. The relationship between D_q, n and D_0 is as following equation.

$$D_q = D_0 \log_e n \tag{2.6}$$

The multi-target survival curves have proved useful for describing

mammalian cells at high doses. However, they do not fit well at a lower dose in clinical radiotherapy.

2-2-2. The linear quadratic model

The formula of second-order polynomial fitting with a zero constant term to ensure survival fraction of 1 at zero doses is termed as linear-quadratic (LQ) model. It is not only the simplest formula mathematically but also it can be explained reasonably from the viewpoint of radiobiological mechanisms. Then, we can define the probability (p) of cell survival (S) during irradiation by the following equation (Figure 5).

$$-\ln(S) = \alpha D + \beta D^2 \tag{2.7}$$

$$p(survival) = e^{(-\alpha D - \beta D^2)} \tag{2.8}$$

The explanation of radiobiological mechanisms in LQ model is that the linear component might result from single-track events (SSB) while the quadratic component might arise from the two-track event (DSB). This interpretation supposed from the outcome of a dose-rate effect shows that the dose rate affects cell survivals due to the change of probability of both events (SSB and DSB).

The simple LQ model gives a good description in low dose prescription in a

clinical situation (about 1.5-3 Gy). The shape is determined by the ratio of α and β, which consist of the linear contribution to damage (αD) and quadratic contribution (βD^2). The response curve of cells to high LET radiation such as α particles or carbon-ions is usually a steep and almost exponentially straight line with high α/β ratio.

2-2-3. Tumour control probability (TCP) model

Dose response curves of cells by radiation have a sigmoid function with the incidence of radiation effects tending to zero as the dose tends to zero and tending to 100 percent at large doses. Munro and Gilbert (13) firstly formulated the target-cell hypothesis of tumour control that based on the result of random nature of cell killing by radiation as a probability of tumour cure after irradiation of tumour cells. More accurately, this calculated probability is only related to the average number of clonogens surviving per tumour.

The Poisson distribution is appropriate for many processes involving the counting of random events such an evaluation of radioactivity or the number of tumour cells forming colonies. When describing tumour control probability (TCP), it is the probability of zero surviving clonogens in a tumour

that is of interest. Moreover, that is the zero-order term of the Poisson distribution and if N_0 denotes the number of clonogens per tumour before irradiation and λ (i.e. $e^{(-D/D_0)}$ in equation (2.1) of single target single hit model) denotes the probability of average number of survived clonogens per tumour after irradiation. Therefore, the value of TCP could be predicted from equation (2.9).

$$\mathrm{TCP} = e^{-N_0\lambda} \tag{2.9}$$

Furthermore, if the average number of surviving clonogenic cells per tumour has the negative exponential function of dose, the TCP would be formed sigmoidal response curve as similar to the collective tumour response as shown in Figure 2b. The curve could be explained only by the random nature of cell killing after irradiation. Therefore, the variation of sensitivity of tumours is not be considered. If we replace the simple exponential curve of λ in equation (2.9) to the probability of an average number of survived clonogens per tumour in LQ model as shown in equation (2.8), the standard model of TCP in LQ model is expressed as following equation.

$$\mathrm{TCP} = e^{-N_0 e^{(-\alpha D-\beta D^2)}} \tag{2.10}$$

Here, N_0 means a function of tumour volume and the clonogenic cell

density (i.e. clonogens/cm^3 in the tumour). However, because the model parameter will be influenced by biological and irradiated dose heterogeneity in the tumour, it could not be practically used in clinical situation.

2-2-4. Normal tissue complication probability (NTCP) model

In modern radiotherapy, the development of treatment techniques often makes possible to avoid normal tissues irradiation preferably. However, the optimized strategies have led to non-uniform partial organ irradiation of normal tissues.

The normal tissue complication probability (NTCP) model was proposed by Lyman (14) for prediction of side effect stochastically by radiotherapy as a function of radiation dose in a partial organ volume. According to the model, the NTCP for the normal tissues can be calculated as following equations.

$$\mathrm{NTCP} = \frac{1}{\sqrt{2\pi}} \cdot \int_{-\infty}^{u(D,V)} e^{-\left(-\frac{1}{2}x^2\right)} dx \qquad (2.11)$$

where, the dependence of dose and volume is in the upper limit of the integral.

$$\mathrm{u}(d,V) = \frac{D - D_{50}(V)}{m \cdot D_{50}(V)} \qquad (2.12)$$

The equation of volume dependence of the D_{50} can express as the following relationship.

$$D_{50}(V) = \frac{D_{50}(1)}{V^n} \quad (2.13)$$

A closer inspection of these three equations shows that there are two independent variables, D and V, and three model parameters, m, $D_{50}(1)$ and n. $D_{50}(1)$ is the uniform total radiation dose producing a 50 percent incidence of the specific side effect if the whole organ is receiving this radiation dose. The volume exponent, n, is the volume effect to the radiation dose. The third parameter, m, is inversely related to the steepness of the radiation response curve.

The Lyman's NTCP model assumes that one part of the normal tissue receives a uniform radiation dose while no dose for the rest of them. Therefore, its use should be coupled with a method of reducing the non-uniform dose distribution across the tissue to corresponding effective volume or effective uniform dose (15). Although dosimetric and biological heterogeneity could cause the radiation response curve to be shallower by improvement of irradiation techniques, due to the complexity of the models and the uncertainties in the model parameters, NTCP modeling has not been widely applied to practical radiotherapy.

2-2-5. Steepness of radiation response curves in the tumour and normal

tissues

The most convenient way to quantify the steepness of the radiation response curve is using the 'γ' (i.e. gradient of the curves) proposed by Brahme (16). This measure has a very simple interpretation that the fraction of increase response by irradiated dose. The definition of 'γ' is expressed as following equation.

$$\gamma \approx \lim_{\Delta D \to 0} \frac{P(D+\Delta D)-P(D)}{\Delta D} = D\frac{\Delta P}{\Delta D} = \mathrm{D} \cdot \mathrm{P}'(D) \qquad (2.14)$$

where, $\mathrm{P}(D)$ means the response as a function of dose, and $\Delta\mathrm{D}$ means a small increment in dose. Therefore, 'γ' is multiplier that converts a relative change in dose into a change of TCP by following equation.

$$\Delta P \approx \gamma \cdot \frac{\Delta D}{D} \qquad (2.15)$$

The value of 'γ' depends on the response level typically written with an index indicating the steepness of radiation response curves, usually at the 50 percent level as 'γ_{50}'. However, because the steepness of radiation response curve varies at another level, assuming a fixed value for 'γ' is sensitive to uncertainty for calculation using the TCP/NTCP model.

Chapter 3

Radiosensitivity uncertainty evaluation for the *in vitro* biophysical modeling of EMT6 cells

3.1. INTRODUCTION

Recently, there have been rapid advances in radiotherapy technologies, such as volumetric modulated arc therapy (VMAT), stereotactic body radiotherapy (SBRT), and image-guided radiotherapy (IGRT) (17-21). Because clinical failures after radiation therapy due to hypoxia, intrinsic radioresistance, and cellular proliferation are known to induce genetic changes, radiobiological parameters and molecular biology data from tumour and critical organs could be used in clinical practice for better treatment (22, 23).

Applying biophysical models to treatment planning in radiotherapy, several researchers reported about the feasibility of prediction or evaluation for tumour controllability and toxicity in normal tissues in a clinical situation (24, 25). Radiation sensitivity is usually affected by cell heterogeneity and radiosensitizing agents (26-28). Nevertheless, the uncertainty surrounding

radiosensitivity because of the factors are not well accounted for in biophysical modeling (29, 30). In particular, hypoxic cells in the tumours lead to increased radioresistance of clonogens, which affects the clinical outcome (31, 32). Etanidazole (ETZ) and misonidazole are well known hypoxic cell radiosensitizers but have had limited beneficial impact on radiotherapy because of side effects such as neurotoxicity (33). For biophysical evaluation of physical dose prescriptions, including dose fractions and biologically equivalent dose (BED), the linear-quadratic (LQ) model based on intrinsic radiosensitivity is commonly used in practical radiotherapy (34). However, to make precise predictions on outcomes after radiotherapy for the treatment planning stage, the other uncertainties of radiation sensitivity would need to be carefully considered.

We evaluated the distribution of uncertainty of cell survival due to radiation and assessed the predictions of tumour response using three different *in vitro* experimental cell cultures. We then discussed the relationship between *in vitro* radiosensitizing activities and uncertainties in characteristics of cell survival using radiobiological parameters.

3-2. MATERIALS AND METHODS

3-2-1. Development of the experimental system

In this experimental system, we have synthesized ETZ and have maintained EMT6/KU mouse mammary tumour cells in Eagle's MEM medium (Sigma-Aldrich Japan, Tokyo, Japan) supplemented with 10% fetal bovine serum (JR Scientific, Inc., Woodland, CA, USA) in our laboratory. For single cell experiments, exponentially growing cells were harvested at normoxic cell culture by trypsinization in the dishes, and suspended in test tubes containing 1 ml of E-MEM (2×10^6 cells/ml). In the hypoxic cultures, they were treated with 95% N_2–5% CO_2 gas for 30 min. *In vitro* radiosensitization was also measured in single EMT6/KU cells by adding radiosensitizer under hypoxic conditions.

3-2-2. Radiation procedure

X-ray irradiation was carried out using an X-ray unit (Hitachi X-ray unit, model MBR-1505R2) with 0.5 mm Al and 1.0 mm Cu filter (150 kV, 4 Gy/min). In *in vitro* assays, cells on the dish were irradiated with 4–28 Gy. After irradiation, colony formation assays were performed.

3-2-3. Biophysical modeling

To determine cell survival rate as to tumour control, we use the LQ formalism that reflects the various tumour parameters. The probability of cell survival in colony by single fraction dose is given by equation (3.1),

$$N = N_0 exp(-\alpha D - \beta D^2) \quad (3.1)$$

where N equals the number of surviving cells, N_0 equals the number of tumour cells at the start of the experiment, α and β equal the estimates of radiosensitivity, and D equals the total dose given. Based upon the assumption that the effect of n equally sized fractions and d equally dosed fractions, and if repair of sublethal damage between fractions between fractions is complete and the proliferation during radiation treatment course can be ignored, the above equation (3.1) can transcribe as equation (3.2):

$$N = N_0\{exp(-\alpha d - \beta d^2)\}^n \quad (3.2)$$

here, the effect (E) of multiple fractions in a multidose schedule can be expressed as equation (3.3):

$$E = -\ln\{exp(-\alpha d - \beta d^2)\}^n = n(\alpha d + \beta d^2) \quad (3.3)$$

then, from the relation $D = nd$; the above equation (3.2) and (3.3) can transcribe as equation (3.4) and (3.5):

$$E = (\alpha D + \beta d D) \quad (3.4)$$

$$N = N_0 exp(-E) = N_0 exp(-\alpha D - \beta dD) = N_0 exp\left\{-\alpha D\left(1 + \frac{\beta}{\alpha} d\right)\right\} \quad (3.5)$$

Then, the Poisson probability of there being zero surviving cells at the end of a fractionated treatment course is given as the tumour control probability (TCP) shown in equation (3.6):

$$\text{TCP} = \exp\left[N_0 exp\left\{-\alpha D\left(1 + \frac{\beta}{\alpha} d\right)\right\}\right] \quad (3.6)$$

where TCP equals the tumour control probability; the other parameters are mentioned in equation (3.1) through equation (3.5).

For the evaluation of the radiation sensitivities of different cell cultures, the data obtained from 15, 34, and 21 different cell lines in normoxic, hypoxic, and hypoxic cell culture plus radiosensitizer were analysed respectively. For each cell line, the SF (survival fraction) after a single fraction dose was calculated and entered into the model. Then, the dose survival data for each *in vitro* cell culture experiment was fitted by the model, and biological parameters such as α, β, D_{50}, and γ were determined. A value of D_{50} and γ represented the dose and steepness of a dose-response level on the assumption that survival fraction equals to 0.5, respectively.

3-2-4. Statistical analysis

Exponential regression analyses were used to assess α and β coefficients, respectively. Statistical comparisons of mean values were calculated using a two-sample independent t-test. All the data were analyzed using OriginLab (OriginLab Corporation, Northampton, MA) scientific graphing and statistical analysis software. A *p*-value of less than 0.05 was considered statistically significant.

3-3. RESULTS

3-3-1. Radiation response of the single cell

Figure 6 shows cell survival after single-dose fraction in different cell cultures. In figure 7, fitted curves using median parameter values of the α and β coefficients from exponential regression analysis (solid line and dotted line, respectively), and the effect of each coefficient on the curves (α contribution: dark gray, β contribution: light gray) are presented. As can be seen from these figures, ETZ enhanced the radiosensitivity of EMT6 in a dose-dependent manner under hypoxic conditions. The variations in predicted survival at higher single doses may increase; however, this increase could be suppressed by radiosensitizers.

3-3-2. Comparisons of radiobiological parameters

The radiobiological parameters from these experiments are summarized in Table I. The α parameters (mean ± SD) were 0.257 ± 0.188 Gy^{-1}, 0.078 ± 0.080 Gy^{-1}, and 0.182 ± 0.116 Gy^{-1} in normoxic cell, hypoxic cell, and hypoxic cell plus ETZ cultures, respectively. The β parameters (mean ± SD) were 0.0159 ± 0.0208 Gy^{-2}, 0.0076 ± 0.0113 Gy^{-2}, and 0.0062 ± 0.0077 Gy^{-2}, respectively. The D_{50} parameters (mean ± SD) were 3.2 ± 2.5 Gy, 6.4 ± 2.7 Gy, and 3.7 ± 1.4 Gy, respectively. The α and D_{50} values were significantly different between the normoxic cell culture and hypoxic cell culture ($p < 0.01$), respectively.

3-3-3. Effects of cell survival and tumour control probability on variation in radiobiological parameters

Figure 7 shows that when the α coefficient values fix (light gray), the variations in cell survival curves at high doses increase; as a function of the β coefficient values (dark gray) showing a similar trend in all cell cultures. Figure 8A-C demonstrate that the effects of α and β coefficients parameters on tumour control probabilities (gray shaded area). Under hypoxic conditions, the mean values of α and β coefficients were smaller, and the

D_{50} were much higher than under normoxic conditions as shown in Table I. It is apparent that the tumour control probabilities under such conditions were much lower than that at the same dose under normoxic conditions. The number of cells (proxy for tumour size) is another clinical factor of radioresistance, albeit less efficient than the variations of α and β coefficients for detecting early cancer ($N_0 \leq 10^8$) as shown in Figure 8D-F.

3-4. DISCUSSION

The LQ formalism with α and β coefficients provides quantification of radiobiological response, which describes the radiation inactivation of different intrinsic cellular radiosensitivity. However, in clinical situations, some factors such as inappropriate derivation of α/β ratios from single *in vitro* assays, clarification of radiation-induced late effects, and variations in individual α/β ratios might cause unclear interpretation of the results obtained from early-responding and late-responding tissues (35).

Although the α coefficient is relatively constant throughout the interphase of the cell cycle (36), the intra-tumour heterogeneity could cause variations in intrinsic radiosensitivity at a single fraction dose. Our data show that the

variation of the α coefficient was nearly the same as that in previous studies (37). Consequently, it is suggested that the variation in the α coefficient is in the same order as the radiosensitivity exhibited by asynchronous populations. The β coefficient might be relatively invariant, and its contribution to cell death is much smaller at conventionally fractionated treatment (38). However, hypofractionated protocols in which implemented of recent clinical studies, the β coefficient contributes to cell death by quadratic function so that it might not be negligible.

Wide ranges of the α/β ratios, which can lead to a cell-lethal dose, are shown in our study, including a negative value. It appears that a negative β coefficient causes these results, which may cause different sensitivities of the cells in the heterogeneous populations at the high dose region. Moreover, in the curve fitting process, the data is often more complex than that described using the linear quadratic equation. In the case of single very high-dose fraction experiments, the survival curve might be dependent on the experimental conditions.

Figure 6 shows the radiosensitivities in different cell cultures. The hypoxic cells appear twice as radioresistant as normoxic cells at survival

fraction. Intra-tumour hypoxic cells proportions are an important complicating factor in cancer therapy and are an important target for anticancer drug design (39). Our results show that the use of ETZ in hypoxic conditions improved the radiosensitivity of enhancement ratio (ER) of 1.72 at mean survival fraction, a value almost equal to a previous study (40). Hypoxic cells, which represent one source of tumour heterogeneity, can lead to flat response and survival curves with low α coefficient. The effects of the variations of α and β coefficients, if either one fix to the median value, are shown in Figure 7. In hypoxic conditions, the effects of radiosensitizing by ETZ are proved to increase the α coefficient, with a decrease of variations in the α and β coefficients. However, in such conditions, the β coefficient's contribution of radiosensitivity was relatively small. Consequently, the results suggest that ETZ could lead to improvement of tumour heterogeneities at high doses, including the change of oxygen tension and electron affinity.

Figure 8 shows the variations of calculated tumour control probability (TCP) curves accounting for the discrepancies between α and β coefficients and cell numbers (tumour volume). Several authors have pointed out that a

precise prediction could potentially be possible by assuming the distribution of intrinsic radiosensitivity at various cellular circumstances (30, 41). Other important factors for determining the TCP is the number of cells that should be killed to result in a tumour cure; studies have shown a consistent cell density of 0.5–1.0 × 10^6/g (42, 43). Consequently, the number of cells would be in the order of 10^7–10^9 in a typical tumour volume of 0.01–100 ml in clinical settings. Also, non-proliferating tumour cells are considered to be more resistant to radiation than that by proliferating cells (44). Proliferation is a critical factor influencing the TCP, especially at highly fractionated treatment schedules (45). It also could be reasonable to consider that the variations of intrinsic radiosensitivities of cells *in vitro*, tumour cells extracted by biopsy, or the use of tumour-bearing chick embryo (46) could predict the radiation response of like cells *in vivo*. The purpose of this study is not to claim that we fully understand how to model the precise radiation response, but rather to show the relevant biophysical parameters are useful for predicting tumour response.

Chapter 4

Effects of uncertainties of radiosensitivity of biophysical modeling for treatment planning

4-1. Introduction

The components of radiotherapy treatment plan mostly depend on the empirically defined by clinical protocols. In such a situation, the appropriate prescription dose to the tumour, fraction size of the dose, fraction times and irradiation techniques are often determined by evaluating the calculated 3-dimensinal dose distribution and clinical state/staging of each patient.

Development of technological advances in radiotherapy makes possible to improve the radiation dose distribution that enabled fewer patients' toxicity than conventional radiotherapy. However, there have been still clinical failures in radiotherapy at a certain level due to several factors such as radioresistance (47, 48) and limitation of cytotoxic dose to the tumour owing to the damage to the normal tissue (49, 50). Furthermore, the application of more advanced radiotherapy techniques has led to more complex and heterogeneous radiation dose distribution, which may cause to the

intercellular variation of radiation response in the tumour and normal tissues. Ideally, these clinical practices would be desirable to make an accurate prediction for curative intent, while excluding uncertainties of the clinical failures with quantitative approach.

Applying a radiobiological model such as TCP/NTCP model (as described in Chapter2-2-4 to 2-2-5) for radiotherapy is one of the methods to rank several treatment plans. However, the predictive capabilities of current models are still under development (51, 52) because there is still insufficient reliable data on the characteristics of human tissues and tumours in clinical radiotherapy.

The aim of this study was to assess the usefulness of TCP/NTCP model and stochastic biological model applying for Gaussian distribution as the intercellular uncertainty of tumour in the treatment planning.

4.2. Materials and Methods

4-2-1. Application for treatment planning

For biological evaluation in a treatment planning, we used clinical three-dimensional radiotherapy treatment planning system with function of biological evaluation analysis (Eclipse ver.11.0, Varian medical systems, US).

In the planning system, biological parameters such as α/β ratio, γ, D_{50} can be set to any given values to calculate the tumour control probability (TCP) (Figure 9).

4-2-2. Phantom

Firstly, we have prepared a digital voxel phantom of 10 x 10 x 10 cm^3 with a sphere target of 1 cm in diameter placed at a center of the phantom. Then, the dose calculation with a four-field technique was performed (Figure 10a). Secondly, we have simulated a prostate cancer patient of demo data. Then after, the radiation dose calculation with VMAT was performed (Figure 10b).

4-2-3. Beam data

All beam data for calculation of radiation dose distribution used in this study were 6 MV photon beam of Novalis-Tx (BrainLab, US) commissioned for clinical use.

4-2-4. Dose fraction protocols and biologically effective dose

Dose fraction protocols in this analysis were set as below. 70 Gy/35 fr, 72 Gy/36 fr, 74 Gy/37 fr, 76 Gy/38 fr, 78 Gy/39 fr, 72 Gy/40 fr, 73.8 Gy/41 fr, 45.6 Gy/42 fr, 77.4 Gy/43 fr, 79.2 Gy/44 fr, 81 Gy/45 fr, 52.5 Gy/20 fr, 57 Gy/19 fr, 60 Gy/20 fr, 62 Gy/20 fr, 56 Gy/16 fr, 63.2 Gy/20 fr, 66 Gy/22 fr, 35 Gy/5 fr,

37.5 Gy/5 fr and 40 Gy/5 fr of five daily fractions in a week. These dose fraction protocols were divided into three types of group; conventional fractionation (70 Gy/35 fr, 72 Gy/36 fr, 74 Gy/37 fr, 76 Gy/38 fr, 78 Gy/39 fr, 72 Gy/40 fr, 73.8 Gy/41 fr, 45.6 Gy/42 fr, 77.4 Gy/43 fr, 79.2 Gy/44 fr, 81 Gy/45 fr), intermediate hypofractionation (52.5 Gy/20 fr, 57 Gy/19 fr, 60 Gy/20 fr, 62 Gy/20 fr, 56 Gy/16 fr, 63.2 Gy/20 fr, 66 Gy/22 fr), hypofractionation (32.5 Gy/5 fr, 35 Gy/5 fr, 37.5 Gy/5 fr and 40 Gy/5 fr), respectively. As concern to these protocols, we calculated biologically equivalent dose (BED) by the following equation.

$$BED = D\left(1 + \frac{d}{\alpha/\beta}\right) \tag{2.15}$$

where D is the total dose. The parameter d is dose per fraction. BED_3 (often discussed as lower α/β ratio in prostate cancer) and BED_{10} (typical α/β in cancer) are calculated in case the α/β ratio is set to 3 and 10, respectively.

4-2-5. Biological parameters

In all calculation for TCP analysis, we have assumed that the tumour is prostate cancer (clinical stage of B). The default parameters setting of D_{50}, γ, α/β ratio for the stage were 52.7 Gy, 4.2 and 10 Gy, respectively. Also, all

calculation for NTCP analysis were performed as to the grade 2 or greater late rectum toxicity and the grade 3 or greater late bladder toxicity. The default parameters setting of n, m, α/β ratio were 0.29, 0.22 and 3.0 Gy for rectum, and 0.13, 0.11 and 6.0 Gy for bladder, respectively.

4-2-6. Hypothesis of intercellular uncertainties of radiation sensitivity

According to our basic experiments result in our study described in Chapter 3, we hypothesized these biological parameters had Gaussian distribution with a certain amount of range (0 %-50 % for α/β radio and 0 %-30% for other parameters) based on their default value. Then, we have re-evaluated TCP and NTCP variations of the tumour.

4-3. Results

4-3-1. Effects of biologically equivalent dose in clinical protocols

The second and the third column in Table II-IV show BED_{10} and BED_3 of clinical protocols calculated with the α/β ratio of 10 and 3, respectively. Both BED_{10} and BED_3 increase as the higher total dose with the same dose fraction size. However, BED_{10} decreases in high dose fraction size (hypofractionation) at a particular range of total dose, contrary to BED_3 that

increases.

4-3-2. Effects of TCP and NTCP due to biological parameters in clinical protocols

Figure 11 shows variations of tumour control probability (TCP) with calculated BED_{10} of clinical protocols and radiobiological parameters using a digital phantom (a) and a patient data (b).

TCP values mostly depended on the BED_{10} (i.e. irradiated dose to the volume of tumor), which contributed to the cell killing of the tumour directly. As respect to the differences of the α/β ratio, D_{50} and γ value, these parameters slightly affected the TCP (i.e. the lower value of these parameters made the TCP worse, especially in the case of lower BED_{10} both phantom and patient study).

Figure 12 shows variations of normal tissue complication probability (NTCP) with calculated BED_3 of clinical protocols and radiobiological parameters using a patient data as to (a) the rectum and (b) the bladder.

NTCP values mostly depended on the BED_3 (i.e. irradiated dose to the volume of normal tissues), which contributed to the cell killing or cell repairing of the normal tissues directly as to the α/β ratio. As respect to

the differences of n and m value, these parameters strongly affected to the NTCP (i.e. the lower value of n made the NTCP worse, in contrast to the smaller value of m that made the NTCP better, regardless of the value of BED_3 in these clinical protocols).

4-3-3. Variation of TCP and NTCP due to uncertainties of biological parameters

Table II shows The impacts of TCP loss/profit using the Gaussian distributions for radiobiological parameters with patient data. Variations of TCP intricately depended on the clinical protocols and the uncertainties of the parameters. The contributions to the variation of TCP were much higher with the uncertainties of D_{50} rather than that of α/β ratio and γ.

Table III and IV show the impact of NTCP loss/profit using the Gaussian distributions for radiobiological parameters with patient data. Variations of NTCP less depended on the clinical protocols and the uncertainties of the parameters compared to that of TCP. The contributions to the variation of NTCP were much higher as to the bladder than the rectum in a small range. Moreover, these were much affected by the uncertainties of the value of α/β ratio rather than that of the value of m and n in the case of a hypofractionated

protocol with higher total dose.

Our data suggested that these uncertainty effects would be relatively small in conventionally fractionated treatments with 74-78 Gy/35-39 fr or 75.6-81 Gy/45 fr. However, in the case of a hypofractionated protocol such as 40 Gy/5 fr, the effects would be slightly greater in both TCP and NTCP. From these results, the increase of total radiation dose, as well as precise determination of these biological parameters, would minimize these impacts.

4-4. Discussion

A α/β ratio is often used to estimate the effects of radiation on various tissues and compare various dose and clinical protocols. The α/β ratio is defined to be 10 Gy for early-responding tissues and tumour, 3–5 Gy for late responding tissues in clinical situations. However, our study has shown the variation and difference of a α/β ratio, D_{50}, γ in the tumour compared to above fixed value, which has strongly affected by the probability of cell death and cure.

Based on the experimental biological theory, it has been suggested that altered fractionation schemes potentially may have further therapeutic gains.

However, conventionally fractionated treatments often use 1.8 Gy-2 Gy for each fraction and daily 5 times per week has standardized for the administration of acute and late reactions of normal tissues (53). In many clinical situations, a certain amount of total given dose with conventionally fractionated treatments is defined as standard radiotherapy that depends on the treatment site, clinical staging, combined therapy and so on.

In recent clinical studies, the lower α/β ratio of prostate cancer causes much discussion of more efficient treatment such as hypofractionated protocols (54-58). The hypofractionated scheme seemed to have advantages for the variations of α/β ratios in the tumor cells while conventionally fractionated treatments appeared to have disadvantages for the variations of D_{50}. Therefore, conventionally fractionated treatments based on large α/β ratios (=10 Gy) may not be optimal for the prostate cancer treatment protocols. For more precise prediction of such as optimal protocols, tumour control, and normal tissue complication, treatment planning systems should be incorporated TCP and NTCP into the optimization in clinical practice. However, at a low dose per fraction less than 1.0 Gy, the standard LQ model might considerably underestimate the biological effect of a given total dose

because of the DNA repair of the cells (59). Also, a shorter fraction scheme might prevent compensatory proliferation as in acute effects so that it might increase the severity of the normal tissue reactions (60).

Moiseenco reported that the impact of the heterogeneity of prostate cancer cells for low α/β ratio did cause few losses of TCP (61). Xiong et al. reported a similar study to above that the impact of the heterogeneity of prostate cancer patients that assumed for low α/β ratio with different fraction scheme (62). They concluded that the heterogeneity has some effects on hypofractionated treatments for high α/β ratio. However, hypofractionated treatment can be ensured with some extra dose even when the α/β ratio has large errors clinically. There have been some approaches for improved biophysical models instead of LQ model (63-65). However, Shuryak et al. reported that distinct tumoricidal mechanisms do not determine tumor control at hypofractionated protocol (66). Our results also suggested that the heterogeneities of the α/β ratios in the tumour cells might not affect to TCP significantly, except for in case of above mentioned hypofractionated treatments for high α/β ratio.

Whereas, Ray et al. suggested that if the α/β ratios are not accurately

specified and not selected dose fractionations by hypofractionated schedule appropriately, all treatments might increase normal tissue complications unnecessarily (67). Olivotto et al. reported that patients underwent hypofractionated protocol with multiple fractions per day for breast cancer treatments suffered from greater normal tissue toxicity than those in the control protocol (68). Arcangeli et al. also reported that equivalent late toxicity effects between the hypofractionated and conventionally fractionated protocols for prostate cancer treatments and significantly higher freedom from biochemical failure for the hypofractionated protocol (69). Our results also suggested that the heterogeneities of the α/β ratios in the normal tissues especially the rectum and bladder for prostate cancer treatments might affect to increase of NTCP in hypofractionated protocols.

We have challenged to apply these uncertainties for the biological model of prostate cancer treatment protocol in this study. However, there are many factors of uncertainties related to radioresistance such as radiation-induced bystander effect (70, 71), the environment of cell circumstances of hypoxia (39, 72), cancer stem cell (48, 73) and so on.

Chapter 5

Conclusions

In conclusion, our preliminary results have suggested that using the distributions of the biological parameter values in the biophysical modeling, we can evaluate the effects of intercellular radiosensitivity uncertainty for the applications of clinical radiotherapy treatment planning. Further advancement would benefit from additional experiments employing different tumour models, and thus, *in vivo* studies are necessary to develop this modeling. The result from a fundamental study using EMT6 cells, the α coefficient and the dose that killed half of the clonogenes population (D_{50}) were significantly different between the normoxic and the hypoxic cell cultures ($p<0.01$), respectively. The use of radiosensitizers under the hypoxic conditions improved radiosensitivity.

Our data have suggested that the optimal fractionation protocol in the treatment of prostate cancer relates to the value and uncertainties of biological parameters such as α/β ratio, γ, and D_{50}, respectively. Also, it is indicated that the contributions to the variation of TCP were much higher

with the uncertainties of D_{50} rather than that of α/β ratio and γ. Therefore, if α/β ratio of prostate cancer is lower than that of normal tissues such rectum and bladder, hypofractionated protocols that could increase the biologically equivalent dose as compared to standard protocols would result in an improved therapeutic ratio. Our data and several studies showed that hypofractionated schedule treatments with uncertainties of biological parameters might increase normal tissue complications unnecessarily.

However, our study did not mention the factors of uncertainties related to radioresistance such as radiation-induced bystander effect, the environment of cell circumstances of hypoxia, cancer stem cell and so on. Several clinical studies suggested that hypofractionated protocols would have benefit for low α/β ratio tumor such as prostate cancer treatment with capable of reducing normal tissue complication (74, 75). The challenges to apply these uncertainties for the biological model of various clinical protocols are further studies.

Summary

Radiotherapy has developed as primary treatment options for cancer along with surgery and chemotherapy. Recently, more than half of all cancer patients have receiving radiation therapy during their course of illness. Theoretical studies based on the *in vitro* experiments in radiobiology have contributed to the development of radiotherapy. However, few of these still have led to demonstrable clinical gains.

In macroscopic viewpoint, it can be clear that the surviving cells would decrease by a certain amount of radiation dose. In contrast, it is challenging that in microscopic viewpoint, no one still predict which cell die or survive by radiation. These uncertain phenomena would be needed a much more robust and relevant parameter to assess radiation effect stochastically since any cell that retains proliferative capacity can cause failure to cancer treatment.

In this thesis, we investigate the distribution of uncertainty of cell survival due to radiation and application of treatment planning. Firstly, we evaluated the distribution of uncertainty of cell survival due to radiation and

assessed the predictions of tumour response using three different *in vitro* experimental cell cultures with EMT6/KU mouse mammary tumour cells. We then discussed the relationship between *in vitro* radiosensitizing activities with etanidazole (ETZ) and uncertainties in characteristics of cell survival using radiobiological parameters. Secondary, we assessed the usefulness of TCP/NTCP model and stochastic biological model applying for Gaussian distribution as the intercellular uncertainty of tumour in the treatment planning.

The result from a fundamental study using EMT6 cells showed that the α parameters (mean ± SD) were 0.257 ± 0.188 Gy^{-1}, 0.078 ± 0.080 Gy^{-1}, and 0.182 ± 0.116 Gy^{-1} in normoxic cell, hypoxic cell, and hypoxic cell plus ETZ cultures, respectively. The β parameters (mean ± SD) were 0.0159 ± 0.0208 Gy^{-2}, 0.0076 ± 0.0113 Gy^{-2}, and 0.0062 ± 0.0077 Gy^{-2}, respectively. The D_{50} parameters (mean ± SD) were 3.2 ± 2.5 Gy, 6.4 ± 2.7 Gy, and 3.7 ± 1.4 Gy, respectively. The α and D_{50} values were significantly different between the normoxic cell culture and hypoxic cell culture ($p < 0.01$), respectively. The use of radiosensitizers under the hypoxic conditions improved radiosensitivity.

The result from an application study using the treatment planning showed that TCP values mostly depended on the BED_{10} (i.e. irradiated dose to the volume of tumor), which contributed to the cell killing of the tumour directly. NTCP values mostly depended on the BED_3 (i.e. irradiated dose to the volume of normal tissues), which contributed to the cell killing or cell repairing of the normal tissues directly as to the α/β ratio. Our data have suggested that the optimal fractionation protocol in the treatment of prostate cancer relates to the value and uncertainties of biological parameters such as α/β ratio, γ, and D_{50}, respectively. Also, it is indicated that the contributions to the variation of TCP were much higher with the uncertainties of D_{50} rather than that of α/β ratio and γ. However, our study did not mention the factors of uncertainties related to radioresistance such as radiation-induced bystander effect, the environment of cell circumstances of hypoxia, cancer stem cell and so on. Several clinical studies suggested that hypofractionated protocols would have benefit for low α/β ratio tumor such as prostate cancer treatment with capable of reducing normal tissue complication. Our data suggested that these uncertainty effects would be relatively small in conventionally fractionated treatments with 74-78 Gy/35-39 fr or 75.6-81 Gy/45 fr. However,

in the case of a hypofractionated protocol such as 40 Gy/5 fr, the effects would be slightly greater in both TCP and NTCP. From these results, the increase of total radiation dose, as well as precise determination of these biological parameters, would minimize these impacts. Also, our data and several studies showed that hypofractionated schedule treatments with uncertainties of biological parameters might increase normal tissue complications unnecessarily. Therefore, the challenges to applying these uncertainties for the biological model of various clinical protocols are further studies.

Acknowledgment

The work presented in this thesis has performed as a joint project between the College of Life and Materials Systems Engineering, Graduate School of Advanced Technology and Science and the Department of Radiological Technology, Graduate School of Health Sciences, and Department of Radiology at Tokushima University Hospital.

I would like to express my gratitude to all those who have supported me during my Ph.D. studies. In particular, I would like to thank:

Yoshihiro Uto, my primary advisor, for scientific guidance and encouragement throughout these years, and having immense trust in my capacity. I appreciate your kindness and helpful attitude.

Hitoshi Hori, my co-advisor, exciting and rewarding discussions. Your ability to considering research advice is highly worth following.

Motoharu Sasaki, my co-advisor, for helpful comments, and productive discussions and kind support for me. I am grateful for your active assistance in all possible matters, and for always taking your time.

Masahide Tominaga, my co-advisor, for valuable comments, and exciting and rewarding discussions. I am grateful for your active assistance in all possible matters, and for always taking your time.

Yasuo Hara, my co-advisor, for kind support in the work.　I am grateful for your active assistance in all possible matters, and for always taking your time.

Taro Kishi, vice-chief of radiological technologist of Tokushima university hospital and my co-advisor. I am grateful for kind support in the work and active assistance in all possible matters, and for always taking your time.

References

1) Delaney G, Jacob S, Featherstone C, Barton M: The role of radiotherapy in cancer treatment: estimating optimal utilization from a review of evidence-based clinical guidelines. Cancer 104(6): 1129-37, 2005.

2) Baskar R, Lee KA, Yeo R, Yeoh KW: Cancer and radiation therapy: current advances and future directions. Int J Med Sci 9(3): 193-199, 2012.

3) Fowler JF: The linear-quadratic formula and progress in fractionated radiotherapy. Br J Radiol 62(740): 679–694, 1989.

4) Boag JW: The time scale in radiobiology. 12th Failla memorial lecture. Radiat Res Proceedings of the 5th International Congress of Radiation Research 9-29, 1975.

5) Adams GE, Jameson DG: Time effects in molecular radiation biology. Radiat Environ Biophys 17(2): 95-113, 1980.

6) Ellis F: The relationship of biological effect to dosetime-fractionation factors in radiotherapy. In Current Topics in Radiation Research Vol. IV, Ebert and Howard (Eds.). Amsterdam, North Holland. 1968, pp 357-397.

7) Ellis F: Dose, time and fractionation: a clinical hypothesis. Clin Radiol

20(1): 1-7, 1969.

8) Costes SV, Chiolo I, Pluth JM Barcellos-Hoff MH and Jakob B: Spatiotemporal characterization of ionizing radiation induced DNA damage foci and their relation to chromatin organization. Mutat Res 704(1-3): 78-87, 2010.

9) Lewanski CR and Gullick WJ: Radiotherapy and cellular signalling. Lancet Onocol 2(6): 366-370, 2001.

10) Harper JW and Elledge SJ: The DNA damage response: ten years after. Mol Cell 28(5): 739-745, 2007.

11) Kerr JF, Wyllie AH, Currie AR: Apoptosis: a basic biological phenomenon with wide-ranging implications in tissue kinetics. Br J Cancer 26(4): 239–57, 1972.

12) Okada H and Mak TW: Pathways of apoptotic and non-apoptotic death in tumour cells. Nat Rev Cancer 4(8): 592-603, 2004.

13) Munro TR and Gilbert CW: The relation between tumour lethal doses and the radiosensitivity of tumour cells. Br J Radiol 34(4): 246-251, 1961.

14) Lyman JT: Complication probability as assessed from dose-volume histograms. Radiat Res Suppl 8: S13-19, 1985.

15) Seppenwoolde Y, Lebesque JV, de Jaeger K, Belderbos JS, Boersma LJ, Schilstra C, Henning GT, Hayman JA, Martel MK, Ten Haken RK: Comparing different NTCP models that predict the incidence of radiation pneumonitis. Normal tissue complication probability. Int J Radiat Oncol Biol Phys 55(3): 724-735, 2003.

16) Brahme A: Dosimetric precision requirements in radiation therapy. Acta Radiol Oncol 23(5): 379-391, 1984.

17) Oita M, Ohmori K, Obinata K, Kinoshita R, Onimaru R, Tsuchiya K, Suzuki K, Nishioka T, Ohsaka H, Fujita K, Shimamura T, Shirato H, and Miyasaka K: Uncertainty in treatment of head-and-neck tumors by use of intraoral mouthpiece and embedded fiducials. Int J Radiat Oncol Biol Phys 64(5): 1581-1588, 2006.

18) Onimaru R, Shirato H, Shimizu S, Kitamura K, Xu B, Fukumoto S, Chang TC, Fujita K, Oita M, Miyasaka K, Nishimura M and Dosaka-Akita H: Tolerance of organs at risk in small-volume, hypofractionated, image-guided radiotherapy for primary and metastatic lung cancers. Int J Radiat Oncol Biol Phys 56(1): 126-135, 2003.

19) Pardo-Montero J and Fenwick JD: An approach to multiobjective

optimization of rotational therapy. II. Pareto optimal surfaces and linear combinations of modulated blocked arcs for a prostate geometry. Med Phys 37(6): 2606-2616, 2010.

20) Thariat J, Bolle S, Demizu Y, Marcy PY, Hu Y, Santini J, Bourhis J, and Pommier P: New techniques in radiation therapy for head and neck cancer: IMRT, CyberKnife, protons, and carbon ions. Improved effectiveness and safety? Impact on survival? Anticancer Drugs 22(7): 596-606, 2011.

21) Yoshitake T, Nakamura K, Shioyama Y, Sasaki T, Ohga S, Nonoshita T, Terashima K, Asai K, Matsumoto K, and Honda H: Stereotactic body radiation therapy for stage I non-small cell lung cancer patients with chronic respiratory insufficiency requiring domiciliary oxygen therapy. Anticancer Res 32(9): 4041-4044, 2012.

22) Eisenmann S, Voigt W, Muller T, and Dempke W: Sequential X-irradiation induced acquired resistance to oxaliplatin but increased sensitivity to cisplatin in two human teratoma cell lines in vitro. Anticancer Res 30(11): 4471-4476, 2010.

23) Hayes M, Lan C, Yan J, Xie Y, Gray T, Amirkhan RH, and Dowell JE: ERCC1 expression and outcomes in head and neck cancer treated with

concurrent cisplatin and radiation. Anticancer Res 31(12): 4135-4139, 2011.

24) El Sharouni SY, Kal HB, and Battermann JJ: Tumour control probability of stage III inoperable non-small cell lung tumours after sequential chemo-radiotherapy. Anticancer Res 25(6C): 4655-4661, 2005.

25) Gluck I, Vineberg KA, Ten Haken RK, and Sandler HM: Evaluating the relationships between rectal normal tissue complication probability and the portion of seminal vesicles included in the clinical target volume in intensity-modulated radiotherapy for prostate cancer. Int J Radiat Oncol Biol Phys 73(2): 334-340, 2009.

26) Masunaga S, Uto Y, Nagasawa H, Hori H, Nagata K, Suzuki M, Kinashi Y, and Ono K: Evaluation of hypoxic cell radio-sensitizers in terms of radio-sensitizing and repair-inhibiting potential. Dependency on p53 status of tumor cells and the effects on intratumor quiescent cells. Anticancer Res 26(2A): 1261-1270, 2006.

27) Seiz M, Kohlhof P, Brockmann MA, Neumaier-Probst E, Hermes P, A VOND, Vajkoczy P, Schmieder K, and Tuettenberg J: First experiences with low-dose anti-angiogenic treatment in gliomatosis cerebri with signs of angiogenic activity. Anticancer Res 29(8): 3261-3267, 2009.

28) Yamazaki H, Nakamura S, Nishimura T, Kodani N, Tsubokura T, Kimoto T, Sihomi H, Aibe N, Yoshida K, Koizumi M, and Kagiya T: Hypofractionated stereotactic radiotherapy with the hypoxic sensitizer AK-2123 (sanazole) for reirradiation of brain metastases: a preliminary feasibility report. Anticancer Res 33(4): 1773-1776, 2013.

29) Dasu A, Toma-Dasu I, and Fowler JF: Should single or distributed parameters be used to explain the steepness of tumour control probability curves? Phys Med Biol 48(3): 387-397, 2003.

30) Gong J, Dos Santos MM, Finlay C, and Hillen T: Are more complicated tumour control probability models better? Math Med Biol 30(1): 1-19, 2013.

31) Hall EJ, Astor M, Bedford J, Borek C, Curtis SB, Fry M, Geard C, Hei T, Mitchell J, Oleinick N, Rubin J, Tu A, Ullrich R, Waldren C, and Ward J: Basic radiobiology. Am J Clin Oncol 11(3): 220-252, 1988.

32) Harada H: How can we overcome tumor hypoxia in radiation therapy? J Radiat Res 52(5): 545-556, 2011.

33) Brown JM, Diehn M, and Loo BW, Jr.: Stereotactic ablative radiotherapy should be combined with a hypoxic cell radiosensitizer. Int J Radiat Oncol Biol Phys 78(2): 323-327, 2010.

34) Lee SP, Leu MY, Smathers JB, McBride WH, Parker RG, and Withers HR: Biologically effective dose distribution based on the linear quadratic model and its clinical relevance. Int J Radiat Oncol Biol Phys 33(2): 375-389, 1995.

35) Brenner DJ, Sachs RK, Peters LJ, Withers HR, and Hall EJ: We forget at our peril the lessons built into the alpha/beta model. Int J Radiat Oncol Biol Phys 82(4): 1312-1314, 2012.

36) Biade S, Stobbe CC, and Chapman JD: The intrinsic radiosensitivity of some human tumor cells throughout their cell cycles. Radiat Res 147(4): 416-421, 1997.

37) Deacon J, Peckham MJ, and Steel GG: The radioresponsiveness of human tumours and the initial slope of the cell survival curve. Radiother Oncol 2(4): 317-323, 1984.

38) Chapman JD: Can the two mechanisms of tumor cell killing by radiation be exploited for therapeutic gain? J Radiat Res 55(1): 2-9, 2014.

39) Heddleston JM, Li Z, Lathia JD, Bao S, Hjelmeland AB, and Rich JN: Hypoxia inducible factors in cancer stem cells. Br J Cancer 102(5): 789-795, 2010.

40) Brown JM and Workman P: Partition coefficient as a guide to the development of radiosensitizers which are less toxic than misonidazole. Radiat Res 82(1): 171-190, 1980.

41) Sanchez-Nieto B and Nahum AE: The delta-TCP concept: A clinically useful measure of tumor control probability. Int J Radiat Oncol Biol Phys 44(2): 369-380, 1999.

42) Baker F and Sanger L: The Density of Clonogenic Cells in Human Solid Tumors. Int J Cell Cloning 9(2): 155-165, 1991.

43) West CM, Davidson SE, Roberts SA, and Hunter RD: Intrinsic radiosensitivity and prediction of patient response to radiotherapy for carcinoma of the cervix. Br J Cancer 68(4): 819-823, 1993.

44) Suit HD, Zietman A, Tomkinson K, Ramsay J, Gerweck L, and Sedlacek R: Radiation Response of xenografts of a human squamous-cell carcinoma and a glioblastoma-multiforme - a progress report. Int J Radiat Oncol Biol Phys 18(2): 365-373, 1990.

45) Harting C, Peschke P, Borkenstein K, and Karger CP: Single-cell-based computer simulation of the oxygen-dependent tumour response to irradiation. Phys Med Biol 52(16): 4775-4789, 2007.

46) Abe C, Uto Y, Nakae T, Shinmoto Y, Sano K, Nakata H, Teraoka M, Endo Y, Maezawa H, Masunaga S, Nakata E, and Hori H: Evaluation of the in vivo radiosensitizing activity of etanidazole using tumor-bearing chick embryo. J Radiat Res 52(2): 208-214, 2011.

47) Lomonaco SL, Finniss S, Xiang C, Decarvalho A, Umansky F, Kalkanis SN, Mikkelsen T, Brodie C: The induction of autophagy by gamma-radiation contributes to the radioresistance of glioma stem cells. Int J Cancer 125(3): 717-722, 2009.

48) Rycaj K and Tang DG: Cancer stem cells and radioresistance. Int J Radiat Biol 90(8): 615-621, 2014.

49) Jackson A, Marks LB, Bentzen SM, Eisbruch A, Yorke ED, Ten Haken RK, Constine LS, Deasy JO: The lessons of QUANTEC: recommendations for reporting and gathering data on dose-volume dependencies of treatment outcome. Int J Radiat Oncol Biol Phys 76(3 Supple): S155-160, 2010.

50) Grimm J, LaCouture T, Croce R, Yeo I, Zhu Y, Xue J: Dose tolerance limits and dose volume histogram evaluation for stereotactic body radiotherapy. J Appl Clin Med Phys 12(2): 3368, 2011.

51) Jeong J, Shoghi KI, Deasy JO: Modelling the interplay between

hypoxia and proliferation in radiotherapy tumour response. Phys Med Biol 58(14): 4897-4919, 2013.

52) Deasy JO, Mayo CS, Orton CG: Treatment planning evaluation and optimization should be biologically and not dose/volume based. Med Phys 42(6): 2753-2756, 2015.

53) Withers HR: Biologic basis for altered fractionation schemes. Cancer 55(9): 2086-2095, 1985.

54) Brenner DJ and Hall EJ: Fractionation and protraction for radiotherapy of prostate carcinoma. Int J Radiat Oncol Biol Phys 43(5): 1095-1101, 1999.

55) Fowler J, Chappell R, Ritter M: Is alpha/beta for prostate tumors really low? Int J Radiat Oncol Biol Phys 50(4): 1021-1031, 2001.

56) Proust-Lima C, Taylor JM, Sécher S, Sandler H, Kestin L, Pickles T, Bae K, Allison R, Williams S: Confirmation of a low α/β ratio for prostate cancer treated by external beam radiation therapy alone using a post-treatment repeated-measures model for PSA dynamics. Int J Radiol Biol Phys 79(1): 195-201, 2011.

57) Dasu A and Toma-Dasu I: Prostate alpha/beta revisited -- an analysis

of clinical results from 14 168 patients. Acta Oncol 51(8): 963-974, 2012.

58) Fowler JF, Toma-Dasu I, Dasu A: Is the α/β ratio for prostate tumours really low and does it vary with the level of risk at diagnosis? Anticancer Res 33(3): 1009-1011, 2013.

59) Joiner MC, Marples B, Lambin P, Short SC, Turesson I: Low-dose hypersensitivity: current status and possible mechanisms. Int J Radiat Oncol Biol Phys 49(2): 379-389, 2001.

60) Fowler JF, Harari PM, Leborgne F, Leborgne JH: Acute radiation reactions in oral and pharyngeal mucosa: tolerable levels in altered fractionation schedules. Radiother Oncol 69(2):161-168, 2003.

61) Moisseenko V: Effect of heterogeneity in radiosensitivity on LQ based isoeffect formalism for low alpha/beta cancers. Acta Oncol 43(5): 499-502, 2004.

62) Xiong W, Li J, Ma CM: Effect of patient variation on standard- and hypo-fractionated radiotherapy of prostate cancer. Phys Med Biol 50(7): 1483-1492, 2005.

63) Guerrero M, Li XA: Extending the linear-quadratic model for large fraction doses pertinent to stereotactic radiotherapy. Phys Med Biol 49(20):

4825-4835, 2004.

64) Guerrero M, Carlone M: Mechanistic formulation of a lineal-quadratic-linear (LQL) model: split-dose experiments and exponentially decaying sources. Med Phys 37(8): 4173-4181, 2010.

65) Park C, Papiez L, Zhang S, Story M, Timmerman RD: Universal survival curve and single fraction equivalent dose: useful tools in understanding potency of ablative radiotherapy. Int J Radiat Oncol Biol Phys 70(3): 847-852, 2008.

66) Shuryak I, Carlson DJ, Brown JM, Brenner DJ: High-dose and fractionation effects in stereotactic radiation therapy: Analysis of tumor control data from 2965 patients. Radiother Oncol 115(3): 327-334, 2015.

67) Ray KJ, Sibson NR, Kiltie AE: Treatment of Breast and Prostate Cancer by Hypofractionated Radiotherapy: Potential Risks and Benefits. Clin Oncol 27(7): 420-426, 2015.

68) Olivotto IA, Whelan TJ, Parpia S, Kim DH, Berrang T, Truong PT, Kong I, Cochrane B, Nichol A, Roy I, Germain I, Akra M, Reed M, Fyles A, Trotter T, Perera F, Beckham W, Levine MN, Julian JA: Interim cosmetic and toxicity results from RAPID: a randomized trial of accelerated partial

breast irradiation using three-dimensional conformal external beam radiation therapy. J Clin Oncol 31(32): 4038-4045, 2013.

69) Arcangeli G, Saracino B, Gomellini S, Petrongari MG, Arcangeli S, Sentinelli S, Marzi S, Landoni V, Fowler J, Strigari L: A prospective phase III randomized trial of hypofractionation versus conventional fractionation in patients with high-risk prostate cancer. Int J Radiat Oncol Biol Phys 78(1): 11-18, 2010.

70) Prise KM and O'Sullivan JM: Radiation-induced bystander signalling in cancer therapy. Nat Rev Cancer 9(5): 351-360, 2009.

71) Shuryak I, Sachs RK, Brenner DJ: Biophysical models of radiation bystander effects: 1. Spatial effects in three-dimensional tissues. Radiat Res 168(6): 741-749, 2007.

72) Lindblom E, Dasu A, Lax I, Toma-Dasu I: Survival and tumour control probability in tumours with heterogeneous oxygenation: a comparison between the linear-quadratic and the universal survival curve models for high doses. Acta Oncol 53(8): 1035-1040, 2014.

73) Diehn M and Clarke MF: Cancer stem cells and radiotherapy: new insights into tumor radioresistance. J Natl Cancer Inst 98(24): 1755-1757,

2006.

74) Liao Y, Joiner M, Huang Y, Burmeister J: Hypofractionation: what does it mean for prostate cancer treatment? Int J Radiol Oncol Biol Phys 76(1): 260-268, 2010.

75) Vogelius IS, Westerly DC, Cannon GM, Bentzen SM: Hypofractionation does not increase radiation pneumonitis risk with modern conformal radiation delivery techniques. Acta Oncol 49(7): 1052-1057, 2010.

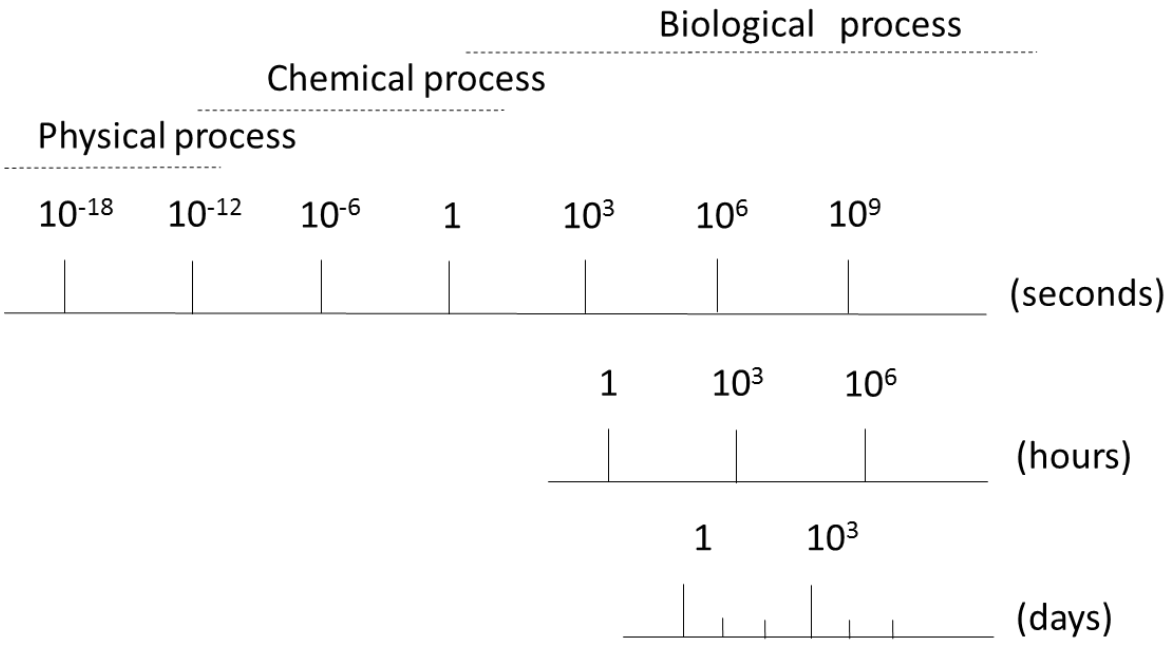

Figure 1. The time frames for effects of radiation.

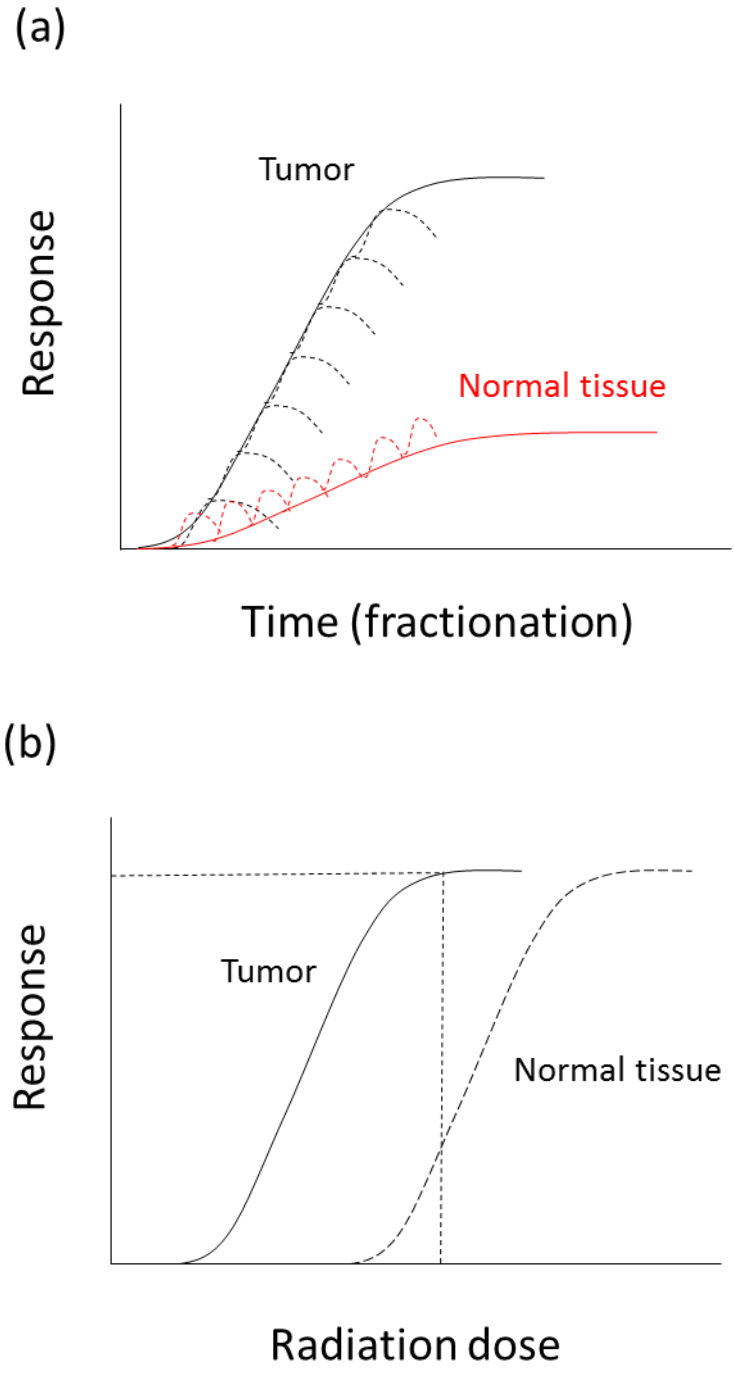

Figure 2. Time-course of radiation response in tumour and normal tissue. (a) The temporal response and (b) the collective response.

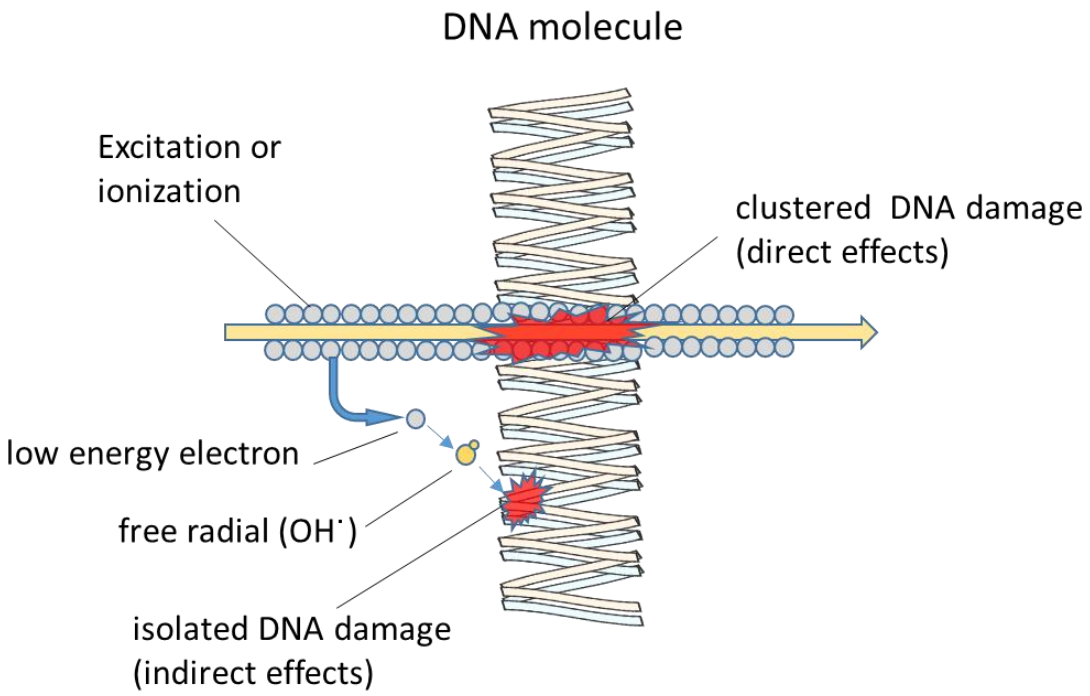

Figure 3. The concept of radiation damage to DNA. Clustered and isolated DNA damage often induce DNA single and double strand breaks.

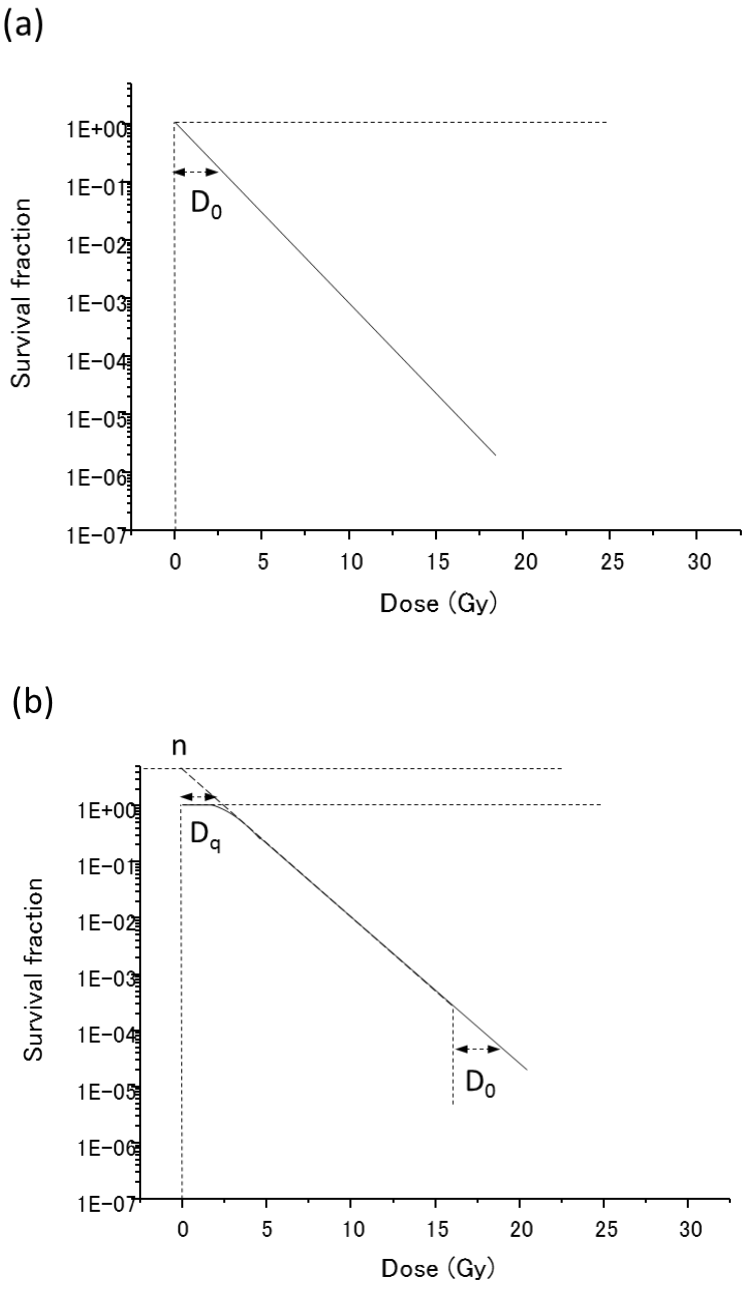

Figure 4. The concept of target theory. (a) single target single hit model. (b)multi-target single hit model.

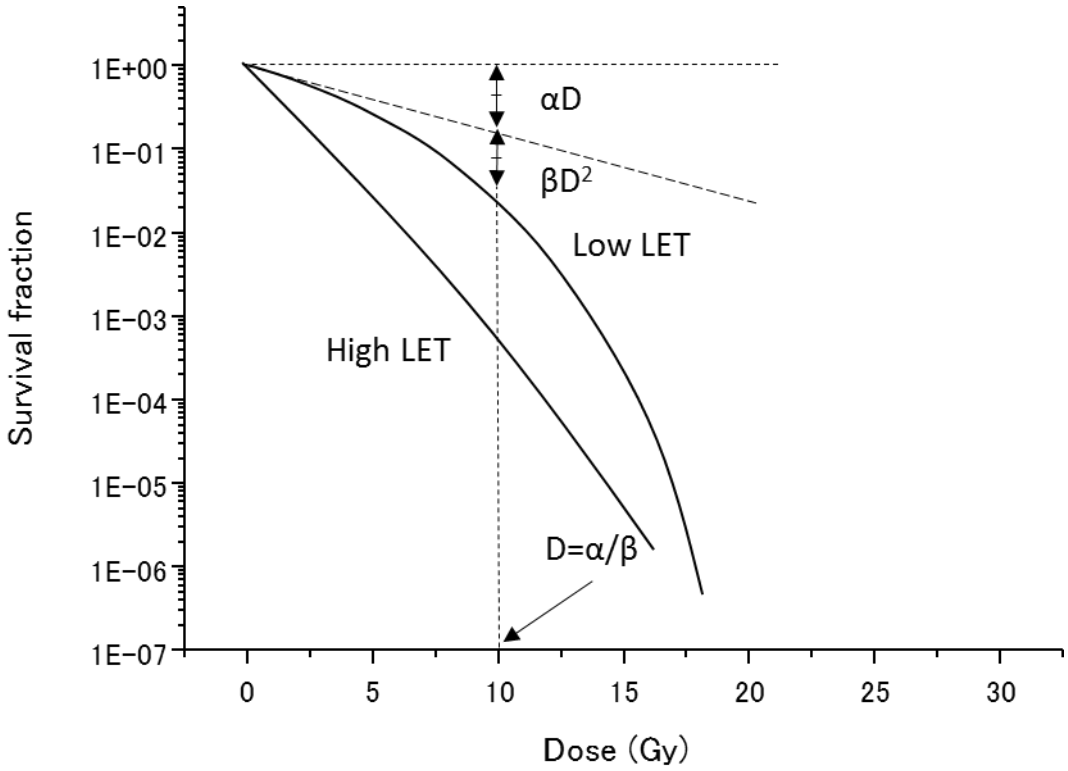

Figure 5. The concept of linear-quadratic (LQ) model.

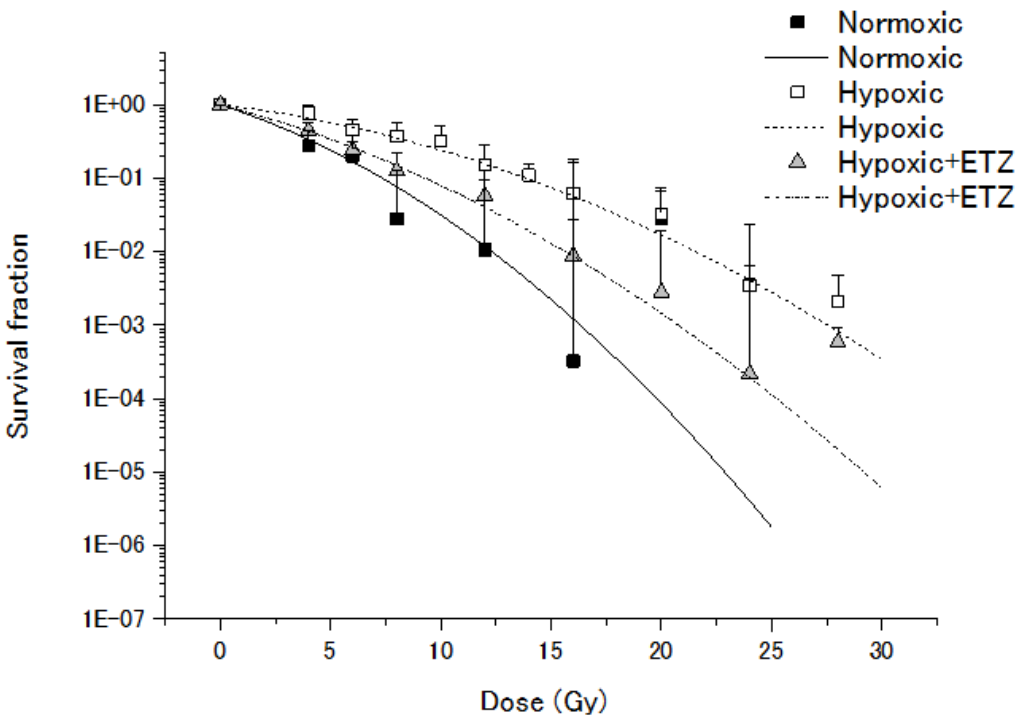

Figure 6. Surviving fractions of EMT6 cells in vitro under normoxia, hypoxia, and hypoxia plus etanidazole (ETZ) culture. Fitted curves (solid line) represent the approximated curves of the α and β coefficients from the exponential regression analysis.

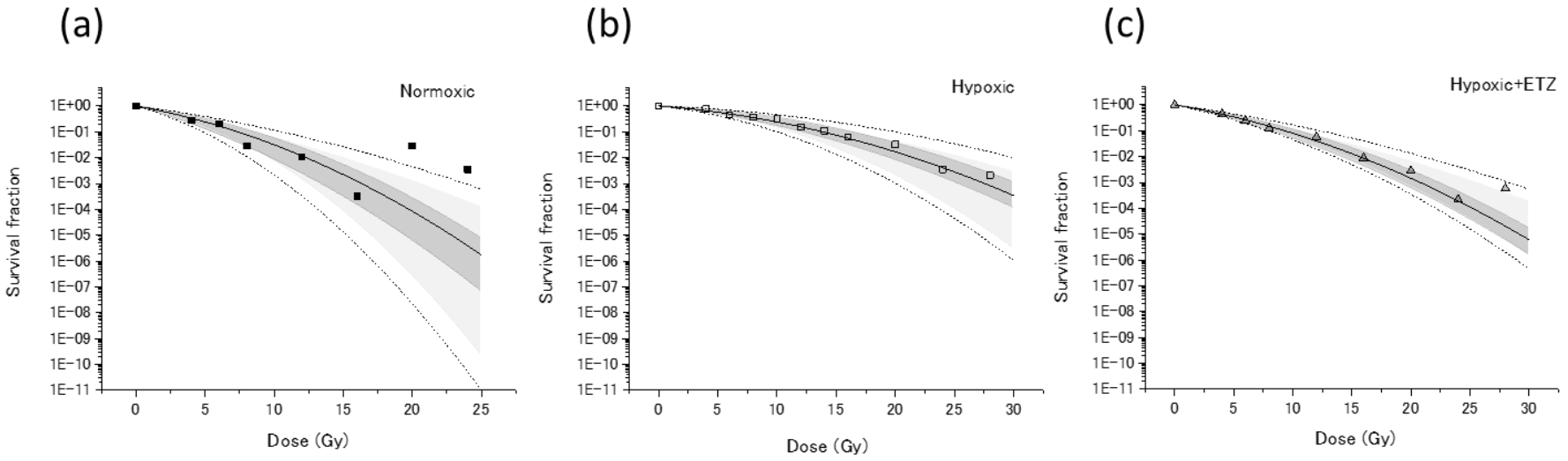

Figure 7. Surviving fractions of EMT6 cells *in vitro* for cells cultured under normoxic (a), hypoxic (b), and hypoxic plus etanidazole (ETZ) (c) conditions. Fitted curves (solid line) represent the approximated curves of the α and β coefficients from exponential regression analysis (solid line and dotted line). The effect of each coefficient on the curves is represented by dark gray shading for the α contribution and by light gray shading for the β contribution with 95% confidence intervals (CI), respectively.

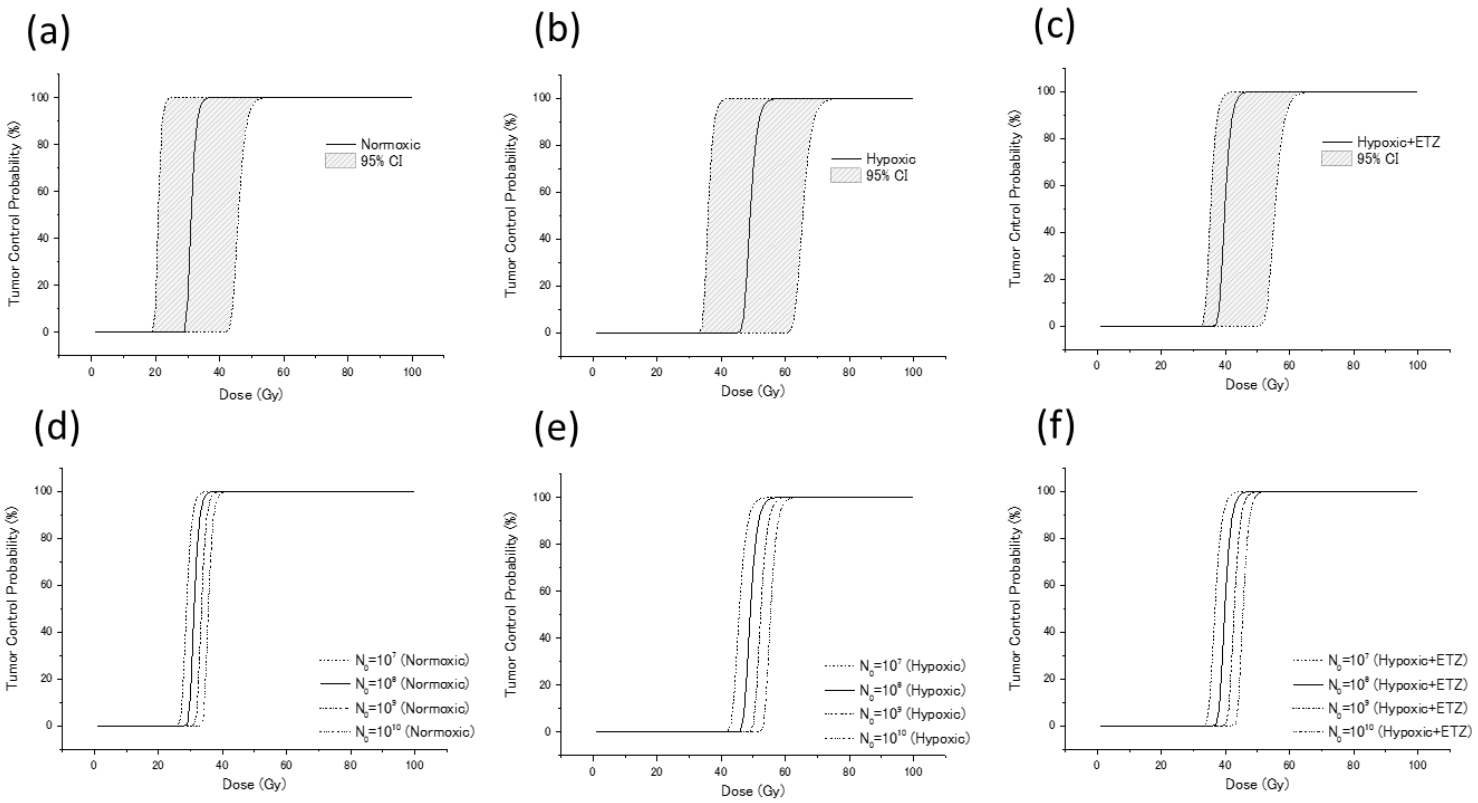

Figure 8. Variations of calculated tumour control probability curves for EMT6 cells *in vitro* for normoxic (a, d), hypoxic (b, e), and hypoxic plus etanidazole (ETZ) (c, f) culture related to the α and β coefficients and cell numbers. Fitted curves (solid line) in a-c represent the approximated curves of the α and β coefficients from exponential regression analysis with 95% confidence intervals (CI) (gray shaded area) in the case of $N_0 = 10^8$, respectively.

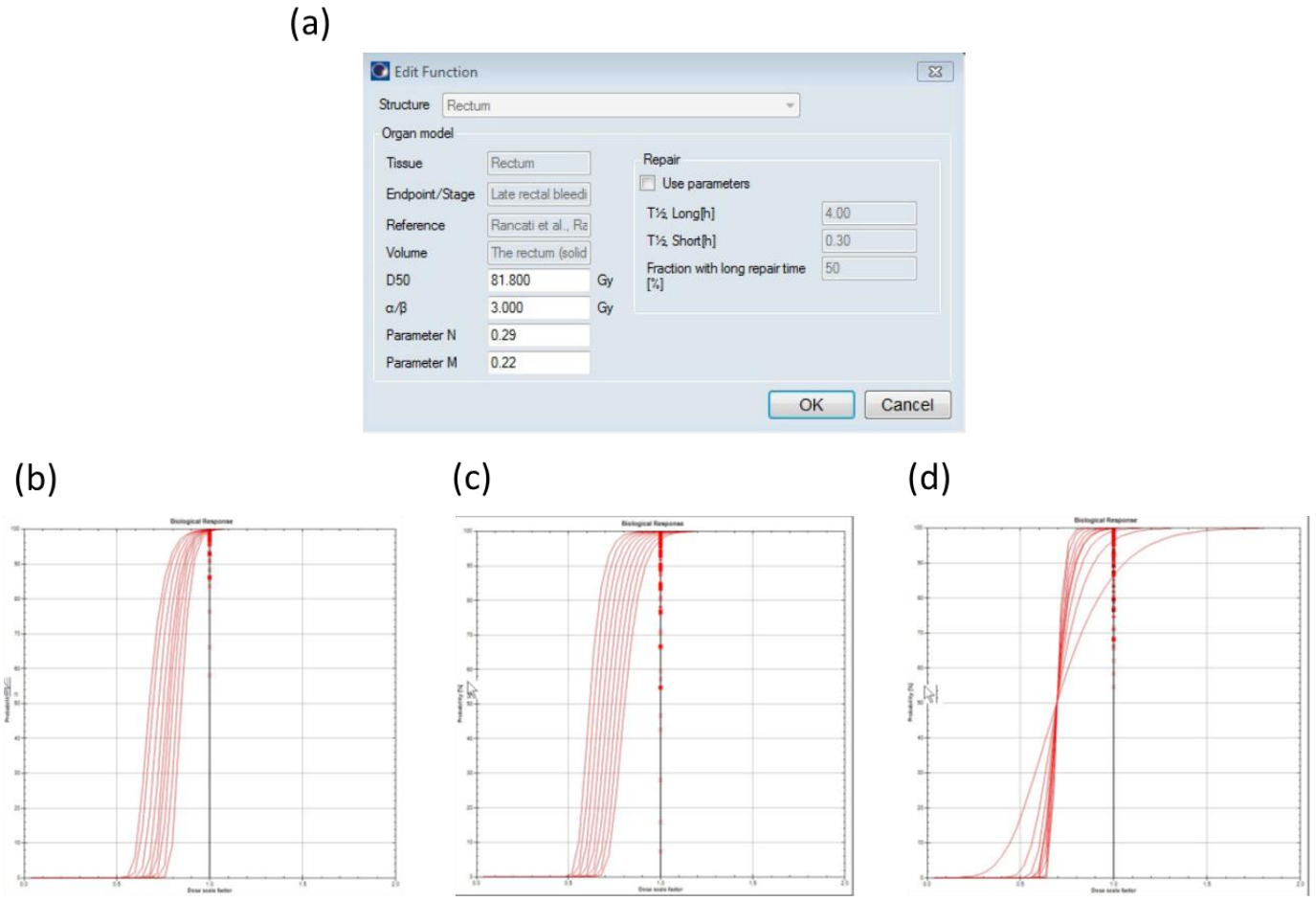

Figure 9. The setting of biological parameters in the treatment planning system(a) and the variations of calculated tumor control probability as respect to (b) α/β ratios, (c) D_{50} values and (d) gamma values.

(a)

(b)

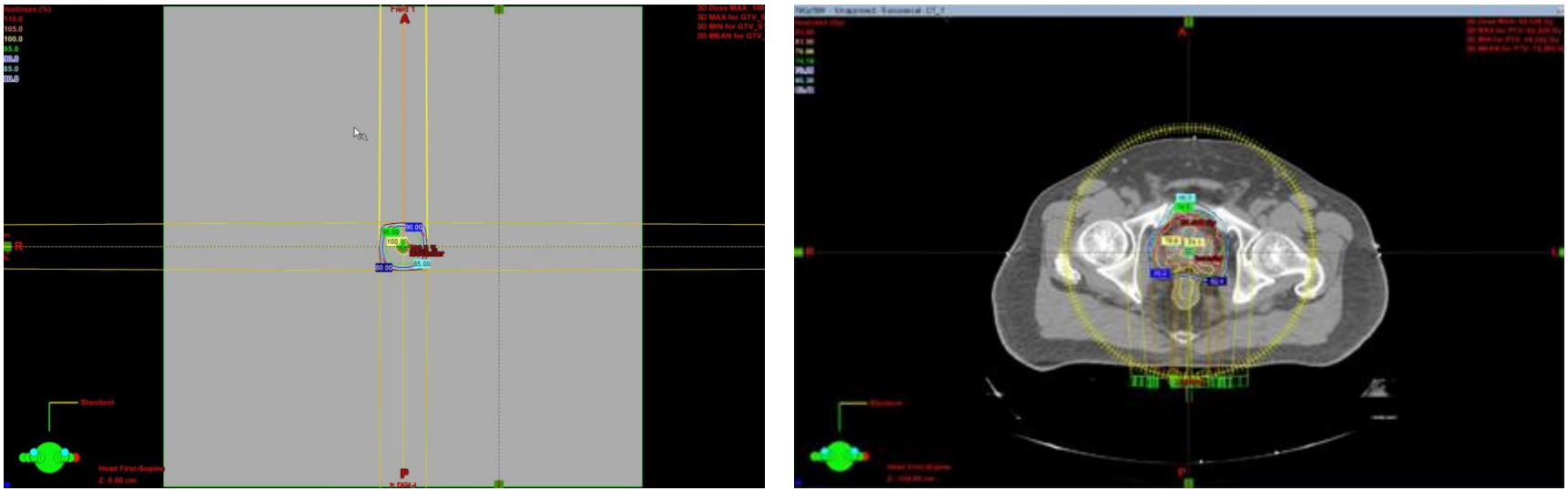

Figure 10. Application for treatment planning by use of a digital phantom (sphere target of φ1cm)(a) and a patient data(b), respectively.

a) Digital phantom

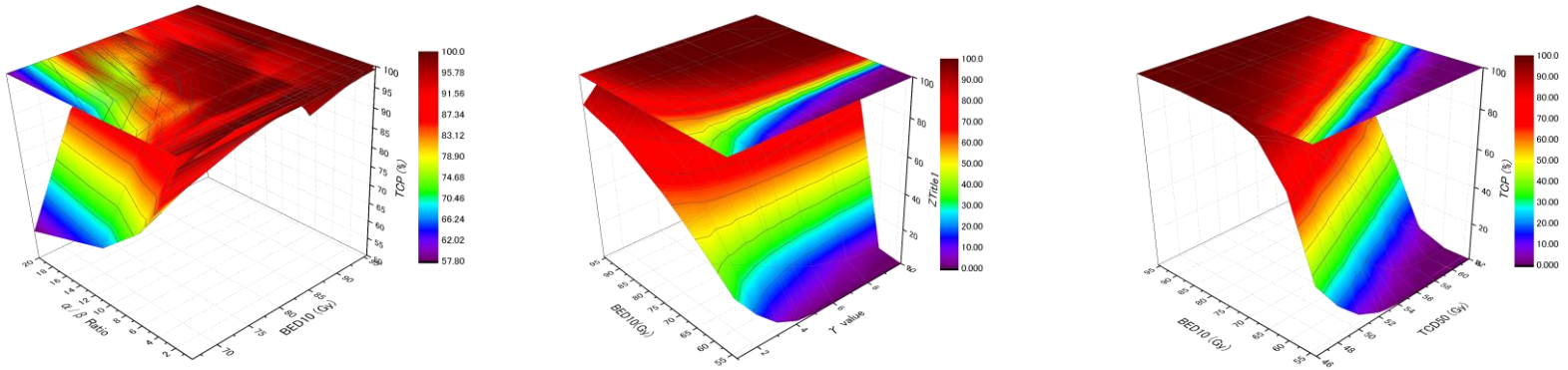

a) Patient data

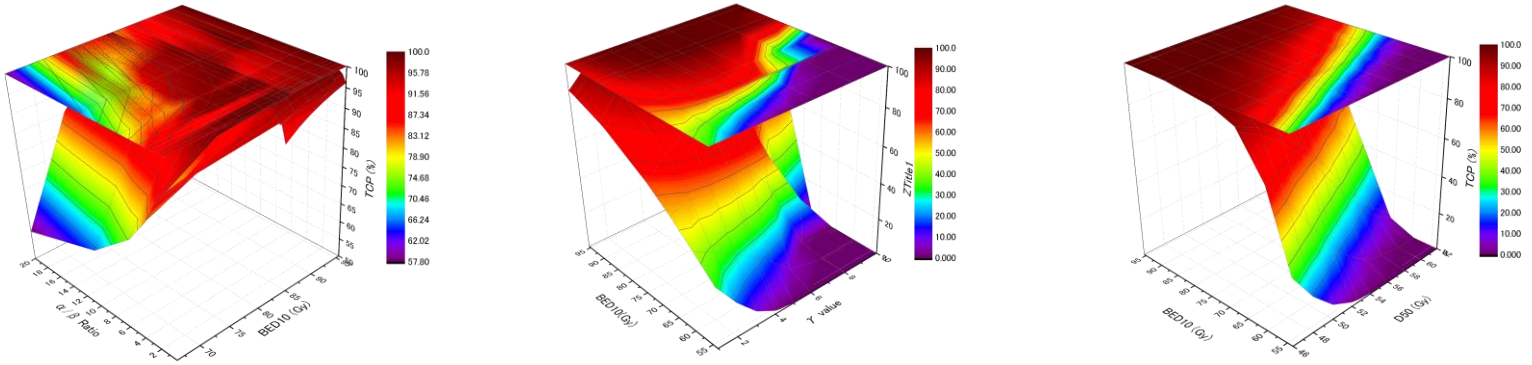

Figure 11. Relationship of tumour control probability between the values of α/β ratio, γ, and D_{50} was evaluated by calculated BED_{10} of each clinical protocols from fraction dose by using a digital phantom(a) and a patient data(b), respectively.

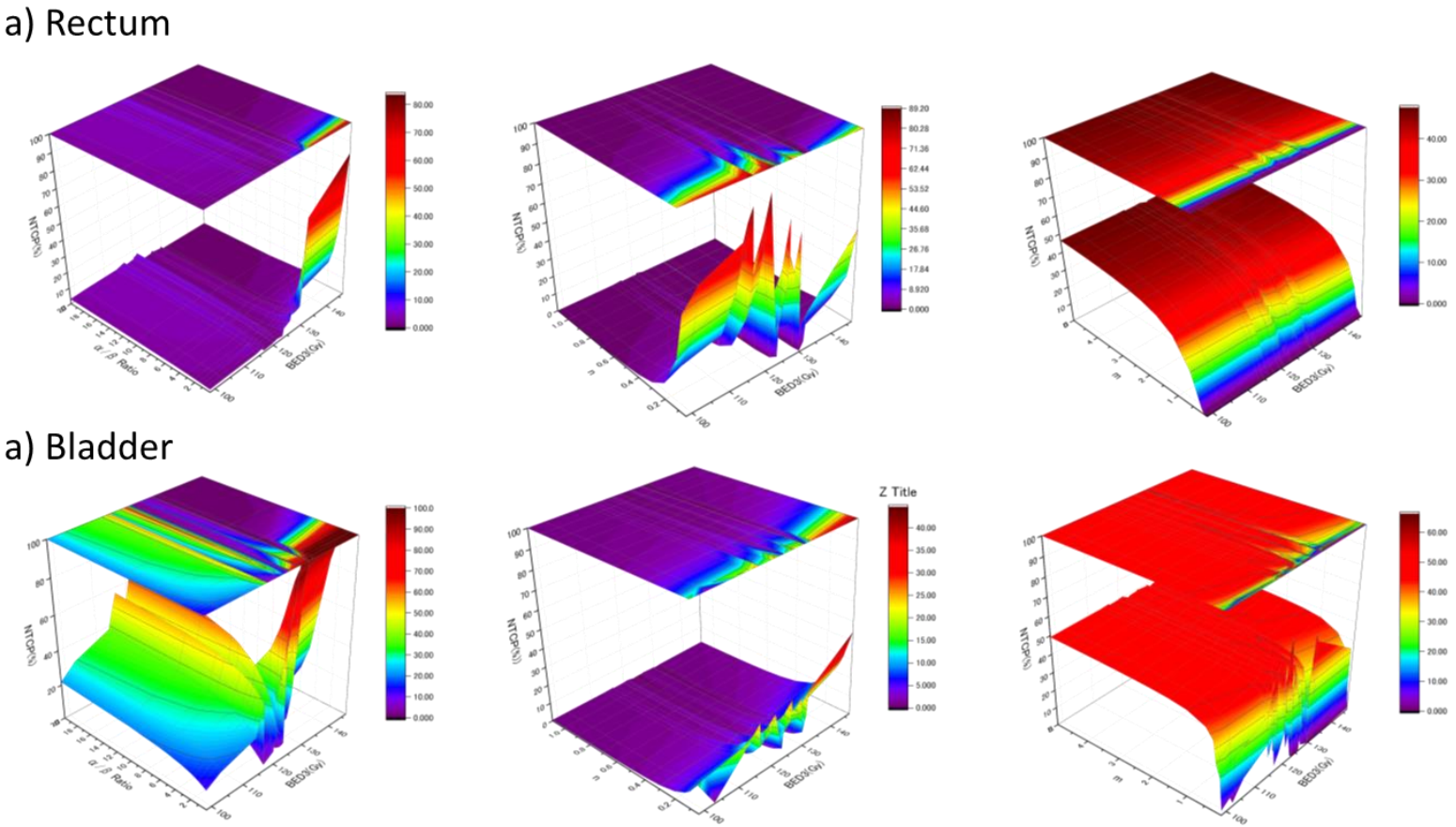

Figure 12. Relationship of normal tissue complication probability between the values of n, m, and α/β ratio was evaluated by calculated BED_3 of each clinical protocols from fraction dose by using a patient data as to (a) the rectum and (b) the bladder.

Table I. Radiobiological parameters of intrinsic *in vitro* radiosensitivity of EMT6 cells. ETZ: Etanidazole. *$p<0.01$ compared to normoxic cell culture.

	Normoxic (n=15)				Hypoxic (n=34)				Hypoxic+ETZ (n=21)			
	Mean	Median	SD	95% CI	Mean	Median	SD	95% CI	Mean	Median	SD	95% CI
α (Gy^{-1})	0.257	0.223	0.188	0.162, 0.351	0.0777*	0.0803	0.113	0.0396, 0.116	0.182	0.179	0.116	0.143, 0.222
β (Gy^{-2})	0.0159	0.0123	0.0208	0.0054, 0.0265	0.0076	0.0062	0.0113	0.0038, 0.0114	0.0062	0.0074	0.0077	0.0036, 0.0088
α/β (Gy)	-12.4	7.8	73.4	-49.5, 24.8	18.1	0.1	114.6	-20.4, 56.7	19.4	20.7	21.9	11.8, 26.9
D_{50} (Gy)	3.21	2.46	2.53	1.93, 4.49	6.44*	6.10	2.71	5.53, 7.35	3.74	3.59	1.35	3.28, 4.21
γ_{50}	1.02	0.79	0.53	0.75, 1.28	1.14	0.92	0.53	0.96, 1.31	0.75	0.78	0.34	0.64, 0.87

Table II. The effects of TCP loss/profit taking into account for the Gaussian distribution for radiobiological parameters compared to fixed value of each parameter at different dose fraction protocols.

TCP diff. compared to fixed value (%)			α/β=10Gy					D50=52.7Gy			γ=4.2		
Dose fraction	BED_{10}(Gy)	BED_3(Gy)	±10%	±20%	±30%	±40%	±50%	±10%	±20%	±30%	±10%	±20%	±30%
70Gy/35fr	84.0	98.4	0.0	0.0	0.0	−0.1	−0.1	−1.5	−6.2	−6.8	−0.2	−0.6	−1.3
72Gy/36fr	86.4	102.9	0.0	0.0	0.0	0.0	−0.1	−1.1	−5.6	−6.2	−0.2	−0.5	−1.1
74Gy/37fr	88.8	114.0	0.0	0.0	0.0	0.0	−0.1	−0.8	−5.2	−5.7	−0.1	−0.4	−1.0
76Gy/38fr	91.2	115.2	0.0	0.0	0.0	0.0	0.0	−0.5	−4.9	−5.4	−0.1	−0.3	−0.8
78Gy/39fr	93.6	116.7	0.0	0.0	0.0	0.0	0.0	−0.4	−4.7	−5.2	−0.1	−0.3	−0.7
72Gy/40fr	85.0	116.7	0.0	−0.1	−0.1	−0.1	−0.2	−1.3	−5.9	−6.5	−0.2	−0.5	−1.2
73.8Gy/41fr	87.1	118.1	0.0	0.0	−0.1	−0.1	−0.2	−1.0	−5.5	−6.0	−0.1	−0.5	−1.1
75.6Gy/42fr	89.2	120.0	0.0	0.0	−0.1	−0.1	−0.1	−0.7	−5.2	−5.7	−0.1	−0.4	−0.9
77.4Gy/43fr	91.3	120.0	0.0	0.0	0.0	−0.1	−0.1	−0.5	−4.9	−5.4	−0.1	−0.3	−0.8
79.2Gy/44fr	93.5	121.0	0.0	0.0	0.0	0.0	−0.1	−0.4	−4.7	−5.2	−0.1	−0.3	−0.7
81Gy/45fr	95.6	121.3	0.0	0.0	0.0	0.0	−0.1	−0.3	−4.6	−5.1	−0.1	−0.2	−0.6
52.5Gy/20fr	66.3	123.3	0.4	0.9	1.4	1.9	2.3	−5.0	−8.2	−9.0	−0.3	−1.0	−2.5
57Gy/19fr	74.1	123.8	0.1	0.3	0.5	0.6	0.7	−4.9	−10.0	−11.0	−0.3	−1.0	−2.3
60Gy/20fr	78.0	126.1	0.1	0.2	0.2	0.3	0.3	−3.3	−8.3	−9.1	−0.3	−0.9	−1.9
66Gy/22fr	85.8	126.7	0.0	0.0	0.1	0.1	0.1	−1.2	−5.8	−6.3	−0.8	−1.3	−1.9
62Gy/20fr	81.2	126.7	0.0	0.1	0.1	0.2	0.2	−2.2	−7.0	−7.7	−0.2	−0.7	−1.6
56Gy/16fr	75.6	129.6	0.1	0.2	0.3	0.4	0.4	−4.3	−9.4	−10.3	−0.3	−1.0	−2.2
63.2Gy/20fr	83.2	129.8	0.0	0.1	0.1	0.1	0.1	−1.7	−6.4	−7.0	−0.2	−0.6	−1.4
32.5Gy/5fr	53.6	130.0	3.5	7.5	11.7	15.5	18.1	7.9	11.4	12.2	0.6	1.5	2.9
35Gy/5fr	59.5	131.3	3.6	7.8	11.4	14.0	15.5	6.6	8.5	8.8	−0.2	−0.5	−0.7
37.5Gy/5fr	65.6	132.0	0.6	1.2	1.6	1.4	0.9	−4.0	−6.7	−7.3	−0.6	−2.0	−4.3
40Gy/5fr	72.0	146.7	−0.9	−1.8	−2.9	−4.1	−5.2	−5.7	−10.5	−11.5	−0.6	−1.8	−4.2

Table III. The effects of NTCP loss/profit taking into account for the Gaussian distribution for radiobiological parameters compared to fixed value of each parameter at different dose fraction protocols as to the rectum.

NTCP diff. compared to fixed value (%)			α/β =3Gy					n=0.29			m=0.22		
Dose fraction	BED_{10}(Gy)	BED_3(Gy)	±10%	±20%	±30%	±40%	±50%	±10%	±20%	±30%	±10%	±20%	±30%
70Gy/35fr	84.0	98.4	0.0	0.0	0.0	0.0	0.0	0.1	0.8	1.1	0.2	0.5	0.9
72Gy/36fr	86.4	102.9	0.0	0.0	0.0	0.0	0.0	0.1	0.9	1.1	0.6	1.3	2.0
74Gy/37fr	88.8	114.0	0.0	0.0	0.0	0.1	0.1	0.2	1.1	1.5	0.0	0.1	0.3
76Gy/38fr	91.2	115.2	0.0	0.0	0.0	−0.1	−0.1	0.2	1.3	1.8	0.4	0.9	1.4
78Gy/39fr	93.6	116.7	0.0	0.0	0.0	−0.1	−0.1	0.2	1.5	2.0	0.4	0.8	1.3
72Gy/40fr	85.0	116.7	0.0	0.0	0.0	−0.1	−0.1	0.1	0.7	1.0	0.1	0.3	0.6
73.8Gy/41fr	87.1	118.1	0.0	0.0	0.0	−0.1	−0.1	0.1	0.8	1.2	0.4	0.8	1.3
75.6Gy/42fr	89.2	120.0	0.0	0.0	−0.1	−0.1	−0.1	0.1	1.0	1.3	0.0	0.1	0.3
77.4Gy/43fr	91.3	120.0	0.0	0.0	−0.1	−0.1	−0.1	0.2	1.1	1.5	0.2	0.5	0.8
79.2Gy/44fr	93.5	121.0	0.0	0.0	−0.1	−0.1	−0.1	0.2	1.3	1.8	0.4	0.8	1.3
81Gy/45fr	95.6	121.3	0.0	0.0	−0.1	−0.1	−0.1	0.2	1.4	2.0	0.6	1.2	1.8
52.5Gy/20fr	66.3	123.3	0.0	0.0	0.0	0.0	0.0	0.0	0.3	0.4	−0.1	−0.2	0.0
57Gy/19fr	74.1	123.8	0.0	0.1	0.1	0.2	0.2	0.1	0.7	1.0	−0.2	−0.4	−0.3
60Gy/20fr	78.0	126.1	0.0	0.1	0.1	0.2	0.3	0.1	0.9	1.3	0.2	0.4	0.8
66Gy/22fr	85.8	126.7	0.1	0.1	0.2	0.4	0.5	0.2	1.6	2.2	−0.6	−1.1	−1.2
62Gy/20fr	81.2	126.7	0.0	0.1	0.2	0.3	0.4	0.2	1.2	1.7	0.1	0.2	0.5
56Gy/16fr	75.6	129.6	0.1	0.1	0.2	0.4	0.5	0.1	1.0	1.4	0.4	0.8	1.3
63.2Gy/20fr	83.2	129.8	0.1	0.1	0.3	0.4	0.5	0.2	1.4	2.0	0.9	1.9	2.7
32.5Gy/5fr	53.6	130.0	0.1	0.1	0.3	0.5	0.7	0.1	0.4	0.5	−0.6	−1.2	−1.4
35Gy/5fr	59.5	131.3	0.1	0.3	0.7	1.2	1.6	0.1	0.8	1.1	−0.3	−0.6	−0.7
37.5Gy/5fr	65.6	132.0	0.3	0.7	1.4	2.4	3.2	0.2	1.5	2.2	0.0	0.1	0.4
40Gy/5fr	72.0	146.7	0.6	1.3	2.5	4.0	5.2	0.4	2.8	3.8	0.9	2.0	2.8

Table IV. The effects of NTCP loss/profit taking into account for the Gaussian distribution for radiobiological parameters compared to fixed value of each parameter at different dose fraction protocols as to the bladder.

NTCP diff. compared to fixed value (%)			α/β =6Gy					n=0.13			m=0.11		
Dose fraction	BED_{10}(Gy)	BED_3(Gy)	±10%	±20%	±30%	±40%	±50%	±10%	±20%	±30%	±10%	±20%	±30%
70Gy/35fr	84.0	98.4	0.0	−0.1	−0.2	−0.4	−0.5	0.7	1.7	2.6	−0.1	−0.4	−1.3
72Gy/36fr	86.4	102.9	−0.1	−0.2	−0.3	−0.5	−0.6	0.7	1.8	2.7	0.5	0.2	−1.1
74Gy/37fr	88.8	114.0	−0.1	−0.2	−0.4	−0.6	−0.7	0.7	1.7	2.5	0.3	−0.1	−1.0
76Gy/38fr	91.2	115.2	−0.1	−0.2	−0.4	−0.6	−0.8	0.7	1.5	2.1	0.0	−0.2	−0.8
78Gy/39fr	93.6	116.7	−0.1	−0.2	−0.5	−0.7	−0.9	0.5	1.1	1.5	0.0	0.0	−0.7
72Gy/40fr	85.0	116.7	−0.1	−0.3	−0.6	−0.9	−1.0	0.7	1.7	2.6	2.9	5.0	−1.2
73.8Gy/41fr	87.1	118.1	−0.1	−0.4	−0.7	−1.1	−1.3	0.7	1.7	2.6	0.6	0.4	−1.1
75.6Gy/42fr	89.2	120.0	−0.2	−0.5	−0.9	−1.3	−1.6	0.7	1.7	2.5	0.3	−0.1	−0.9
77.4Gy/43fr	91.3	120.0	−0.2	−0.5	−1.0	−1.5	−1.9	0.7	1.5	2.2	0.1	−0.1	−0.8
79.2Gy/44fr	93.5	121.0	−0.2	−0.6	−1.1	−1.7	−2.1	0.6	1.3	1.7	0.0	0.0	−0.7
81Gy/45fr	95.6	121.3	−0.2	−0.6	−1.2	−1.8	−2.3	0.4	0.9	1.1	−0.1	0.2	−0.6
52.5Gy/20fr	66.3	123.3	0.0	0.0	0.1	0.2	0.2	0.1	0.2	0.3	0.3	0.7	−2.5
57Gy/19fr	74.1	123.8	0.2	0.5	1.1	1.9	2.5	0.4	1.0	1.6	0.8	1.4	−2.3
60Gy/20fr	78.0	126.1	0.3	0.8	1.7	2.8	3.8	0.6	1.5	2.4	0.8	1.3	−1.9
66Gy/22fr	85.8	126.7	0.5	1.4	2.6	3.9	4.9	0.8	1.8	2.7	0.3	−0.1	−1.9
62Gy/20fr	81.2	126.7	0.4	1.3	2.5	4.0	5.1	0.7	1.8	2.8	0.7	0.7	−1.6
56Gy/16fr	75.6	129.6	0.4	1.2	2.6	4.3	5.8	0.5	1.3	2.2	0.8	1.4	−2.2
63.2Gy/20fr	83.2	129.8	0.5	1.5	2.9	4.5	5.7	0.8	1.9	2.9	0.5	0.3	−1.4
32.5Gy/5fr	53.6	130.0	0.0	0.2	0.8	2.1	3.4	0.0	0.0	0.1	0.1	0.2	2.9
35Gy/5fr	59.5	131.3	0.2	1.1	3.1	5.8	8.2	0.1	0.2	0.4	0.3	0.6	−0.7
37.5Gy/5fr	65.6	132.0	1.0	3.7	7.7	11.7	14.5	0.3	0.9	1.5	0.7	1.3	−4.3
40Gy/5fr	72.0	146.7	2.4	6.6	11.2	14.7	16.9	0.8	2.0	3.1	0.8	1.0	−4.2

Research Achievement

Peer-reviewed papers

[1] Masataka Oita, Yoshihiro Uto, Masahide Tominaga, Motoharu Sasaki, Yasuo Hara, Taro Kishi, Hitoshi Hori. Radiosensitivity uncertainty evaluation for the In Vitro biophysical modeling of EMT6 cells. Anticancer Research, 34(6):4621-4626, 2014.

[2] Masataka Oita, Yoshihiro Uto, Masahide Tominaga, Motoharu Sasaki, Hitoshi Hori. Effects of uncertainties of radiation sensitivity of biological modelling for treatment planning. Medical Physics, 41(6):256, 2014.

Reviews

[3] Masataka Oita, Yoshihiro Uto, Hideki Aoyama. Moving toward multi-dimensional radiotherapy and the role of radiobiology. Radiation Biology Research Communications, 49(4):358-372, 2014.

Presentations

[4] 笈田将皇，宇都義浩，堀均，富永正英，佐々木幹治，岸太郎細胞間放射線感受性の違いを考慮した最適放射線治療計画法に関する検討，第 17 回バイオ治療

法研究会，福岡市，2013 年 12 月 7 日.

[5] 笈田将皇，宇都義浩，堀均，富永正英，佐々木幹治，岸太郎．細胞間放射線感受性の違いを考慮した治療計画技術応用に関する基礎的検討，第 16 回癌治療増感研究シンポジウム，奈良市，2014 年 2 月 7－8 日.

[6] Masataka Oita, Yoshihiro Uto, Masahide Tominaga, Motoharu Sasaki, Hitoshi Hori. Effects of uncertainties of radiation sensitivity of biological modelling for treatment planning. AAPM 56th Annual Meeting, Philadelphia, USA, 2014.7.19-23.